



Microstructure-Sensitive Crystal Viscoplasticity for Ni-base Superalloys

(with application to long-term creep-fatigue interactions)

Award DE-FE0011722

August 2013 – August 2017 (including NCE)

Program Manager: Dr. Patcharin Burke

PI: Richard W. Neu

The George W. Woodruff School of Mechanical Engineering

School of Materials Science & Engineering

Georgia Institute of Technology

Atlanta, GA 30332-0405

rick.neu@gatech.edu

University Turbine Systems Research Workshop

Virginia Tech

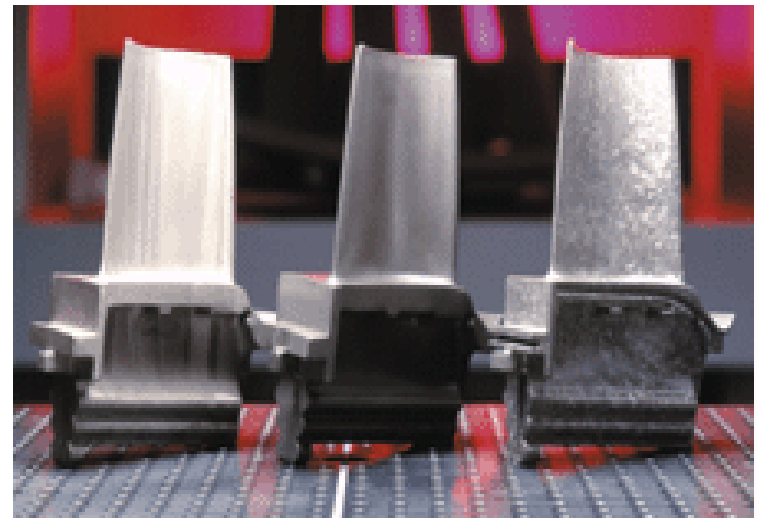
November 1-3, 2016

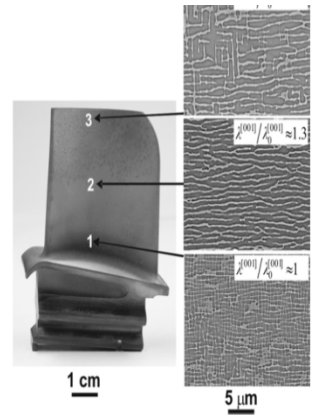


Power Output: 375 MW

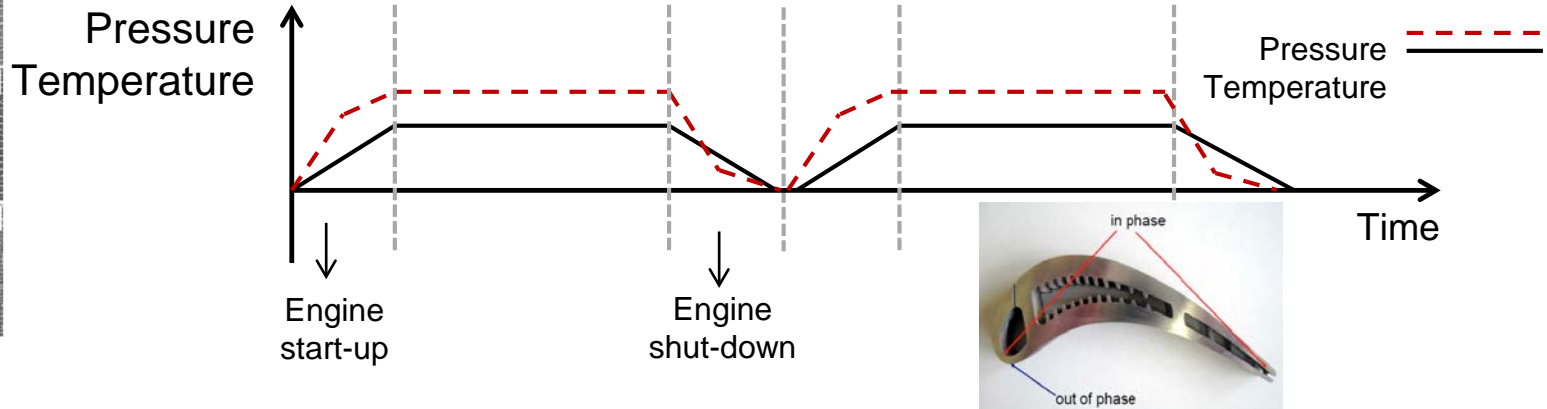
Land-based gas turbines

- drive to increase service temperature to improve efficiency; increase life; with minimal increase in cost
- replace large directionally-solidified Ni-base superalloys with single crystal superalloys

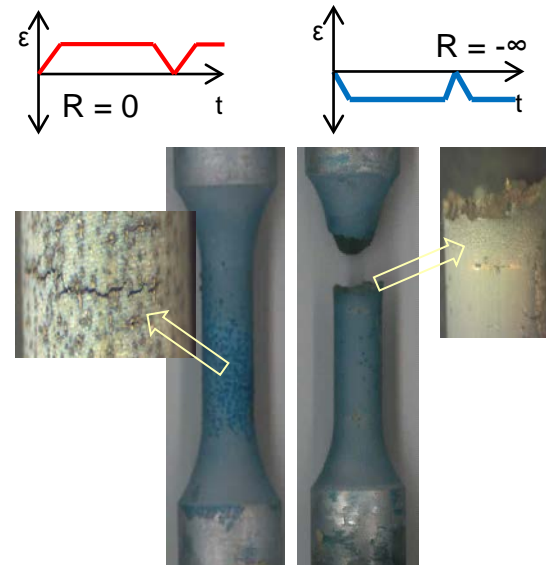
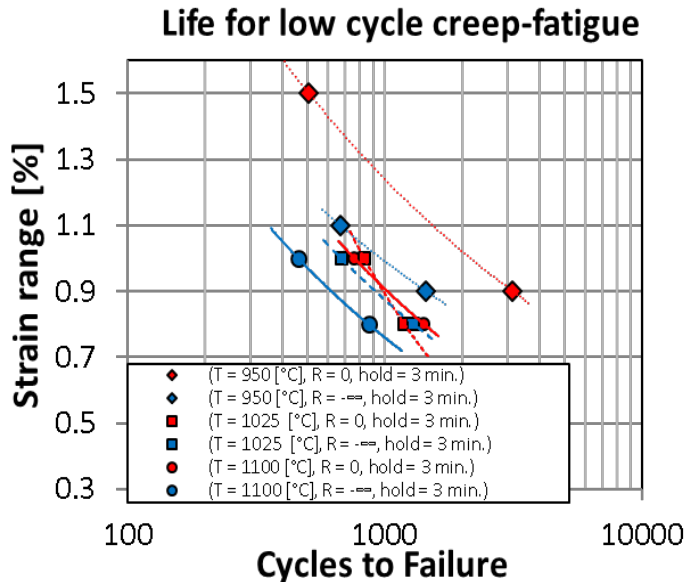




[Epishin et al., 2010]



Superalloys airfoils are subject to a continuation of “process” during service due to sustained hostile environment and loading. Understanding the influence of the microstructure and its evolution on TMF, creep and fatigue and their interactions is key to delivering better turbine designs

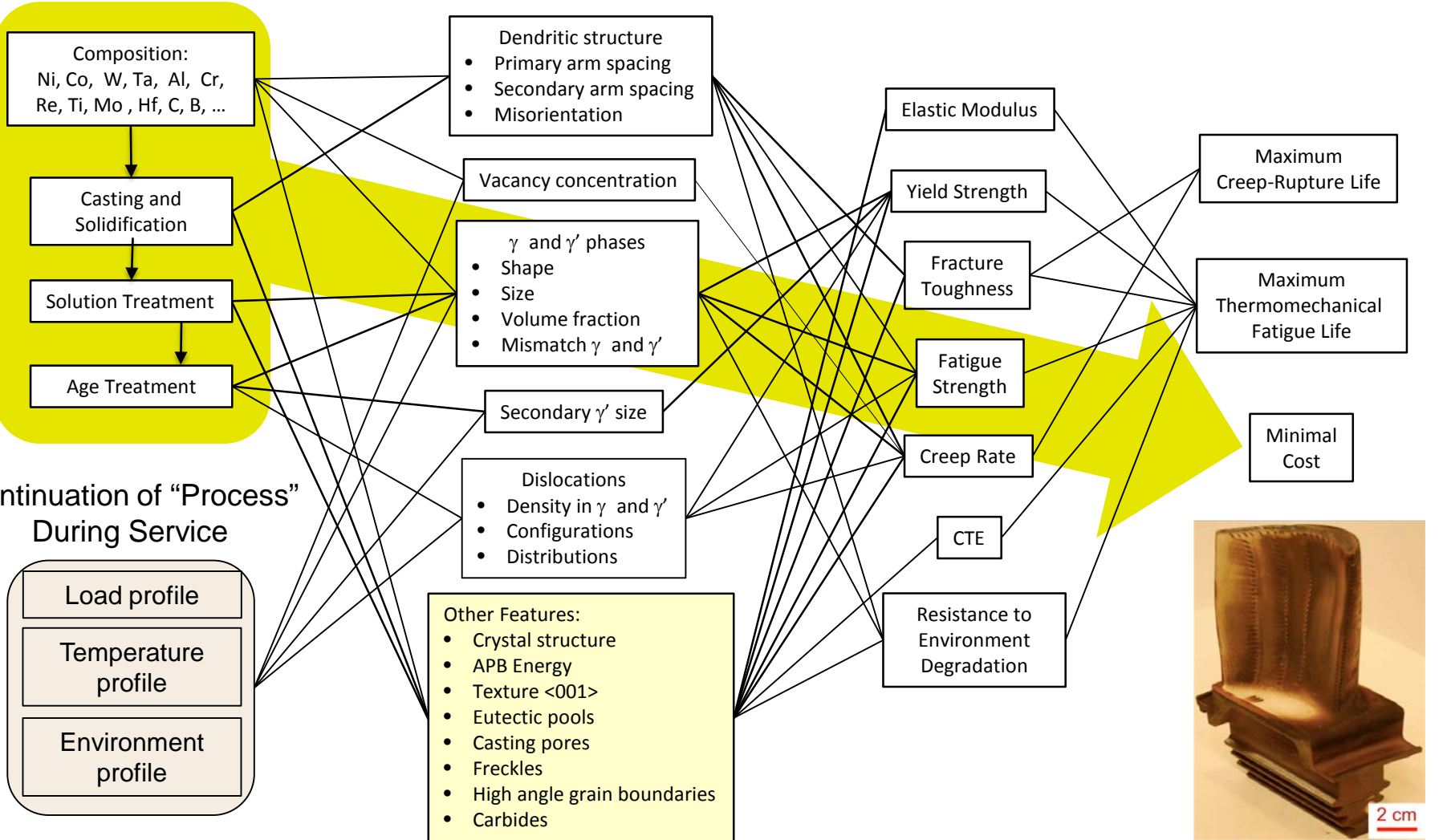


PROCESS

STRUCTURE

PROPERTIES

PERFORMANCE



PROCESS

STRUCTURE

PROPERTIES

PERFORMANCE

Composition:
Ni, Co, W, Ta, Al, Cr,
Re, Ti, Mo, Hf, C, B, ...

Casting and
Solidification

Solution Treatment

Age Treatment

Dendritic structure
• Primary arm spacing
• Secondary arm spacing
• Misorientation

Vacancy concentration

γ and γ' phases
• Shape
• Size
• Volume fraction
• Mismatch γ and γ'

Secondary γ' size

Dislocations
• Density in γ and γ'
• Configurations
• Distributions

Other Features:
• Crystal structure
• APB Energy
• Texture $\langle 001 \rangle$
• Eutectic pools
• Casting pores
• Freckles
• High angle grain boundaries
• Carbides

Elastic Modulus

Yield Strength

Fracture Toughness

Fatigue Strength

Creep Rate

CTE

Resistance to Environment Degradation

Maximum Creep-Rupture Life

Maximum Thermomechanical Fatigue Life

Minimal Cost

Continuation of "Process" During Service

Load profile
Temperature profile
Environment profile



PROCESS

STRUCTURE

PROPERTIES

PERFORMANCE

Composition:
Ni, Co, W, Ta, Al, Cr,
Re, Ti, Mo, Hf, C, B, ...

Casting and
Solidification

Solution Treatment

Age Treatment

Dendritic structure

- Primary arm spacing
- Secondary arm spacing
- Misorientation

Vacancy concentration

γ and γ' phases

- Shape
- Size
- Volume fraction
- Mismatch γ and γ'

Secondary γ' size

Dislocations

- Density in γ and γ'
- Configurations
- Distributions

Other Features:

- Crystal structure
- APB Energy
- Texture $\langle 001 \rangle$
- Eutectic pools
- Casting pores
- Freckles
- High angle grain boundaries
- Carbides

Elastic Modulus

Yield Strength

Fracture Toughness

Fatigue Strength

Creep Rate

CTE

Resistance to Environment Degradation

Maximum Creep-Rupture Life

Maximum Thermomechanical Fatigue Life

Minimal Cost

Continuation of "Process" During Service

Load profile

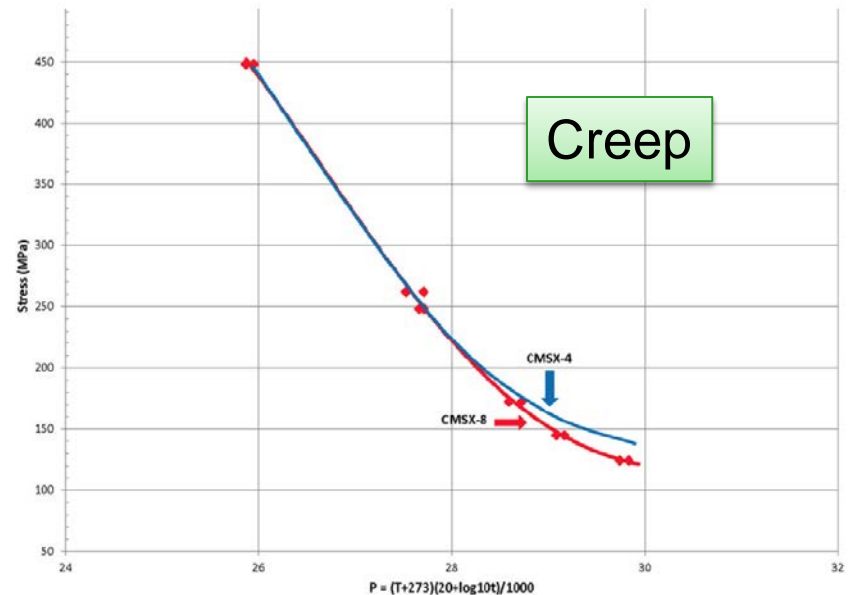
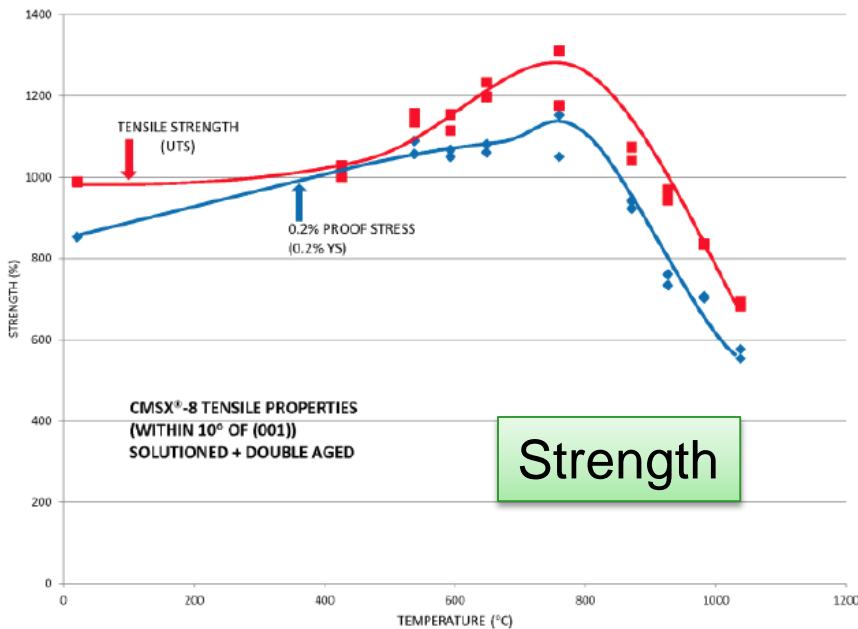
Temperature profile

Environment profile

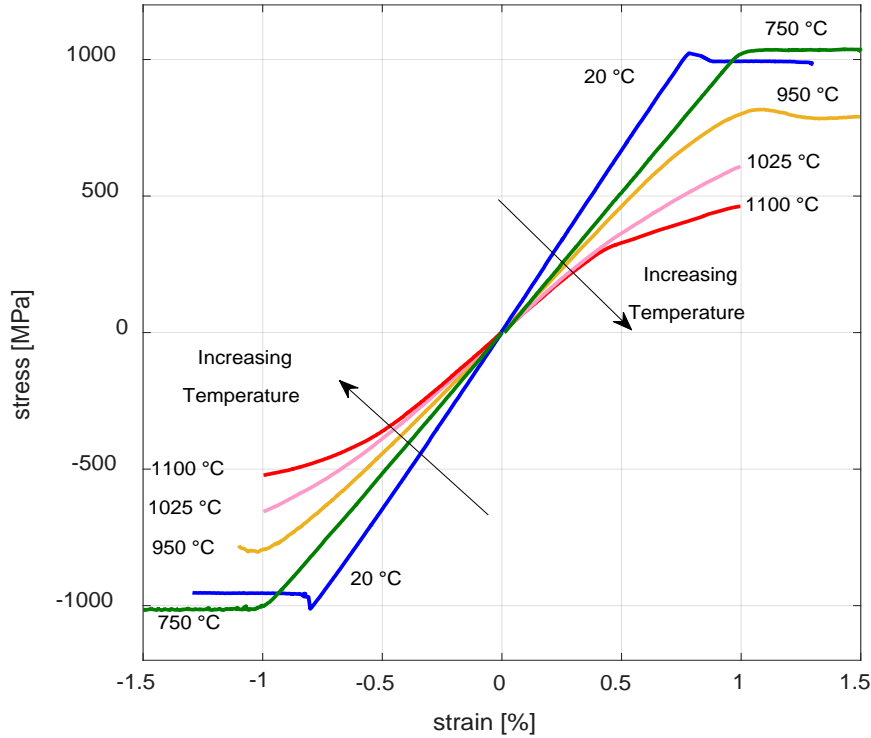


CMSX-8: 1.5% Re "alternative 2nd gen alloy" replacing 3.0% Re containing alloys (e.g., CMSX-4, PWA1484)

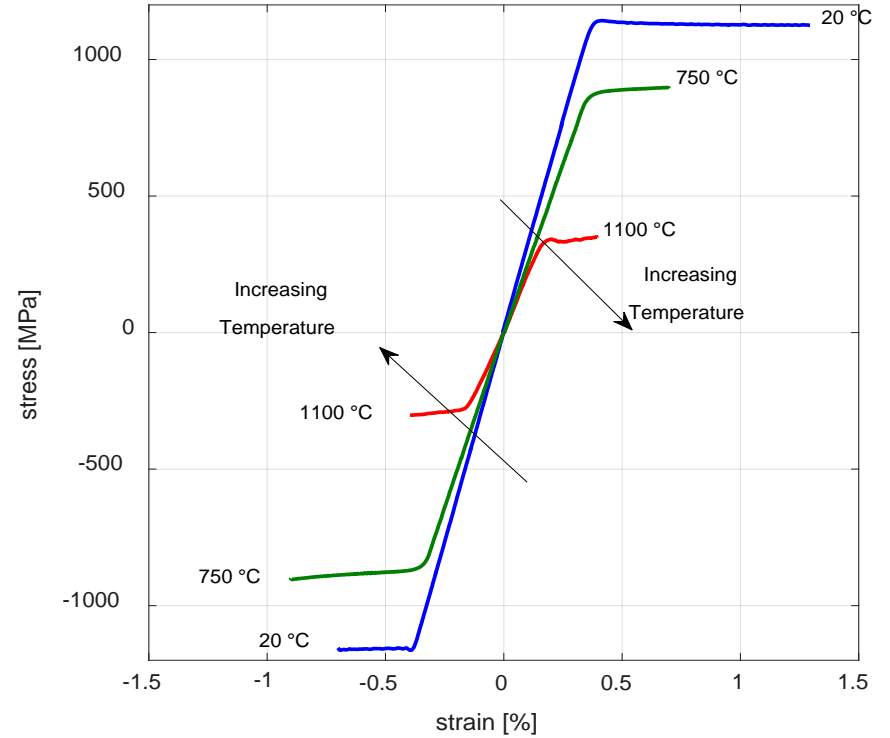
Alloy	Cr	Co	Mo	W	Al	Ti	Ta	Re	Hf	C	B	Zr	Ni
Mar-M247LC-DS	8.4	10.0	0.7	10.0	5.5	1.0	3.0	-	1.5	0.07	0.015	0.05	Bal
CM247LC-DS	8.1	9.2	0.5	9.5	5.6	0.7	3.2	-	1.4	0.07	0.015	0.01	Bal
CMSX-4	6.5	9.0	0.6	6.0	5.6	1.0	6.5	3.0	0.1	-	-	-	Bal
SC16	16	0.17	3.0	0.16	3.5	3.5	3.5	-	-	-	-	-	Bal
PWA1484	5.0	10.0	2.0	6.0	5.6	-	9.0	3.0	0.1	-	-	-	Bal
CMSX-8	5.4	10.0	0.6	8.0	5.7	0.7	8.0	1.5	0.2	-	-	-	Bal



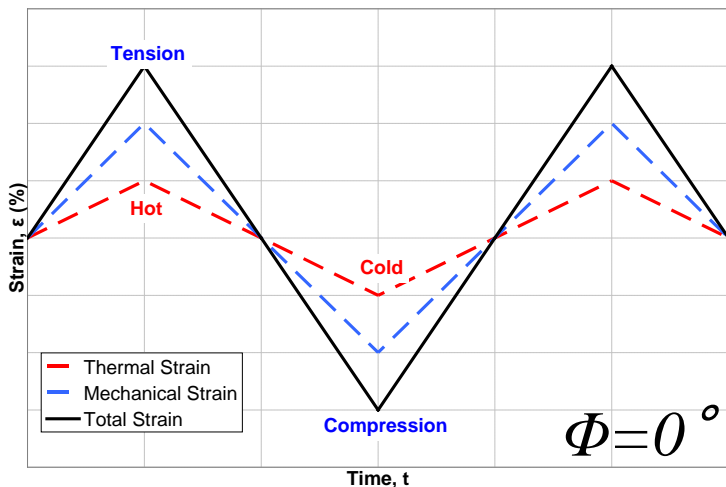
Virgin CMSX-8 monotonic response in the <001> dir



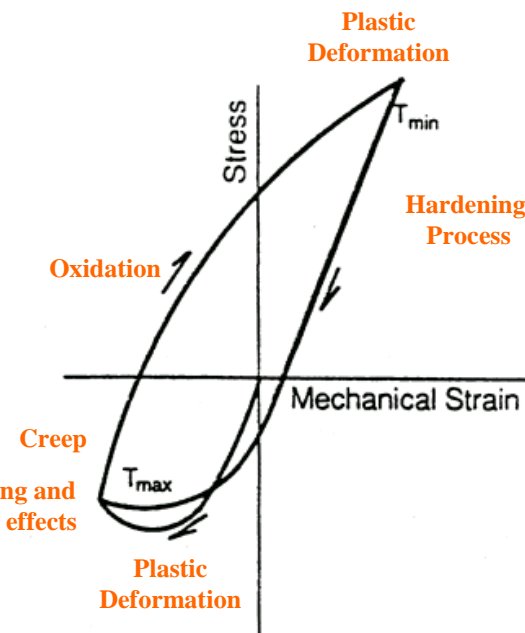
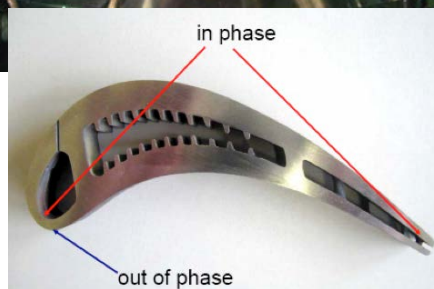
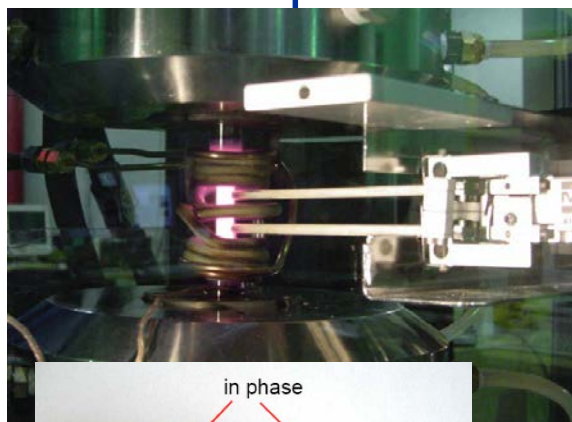
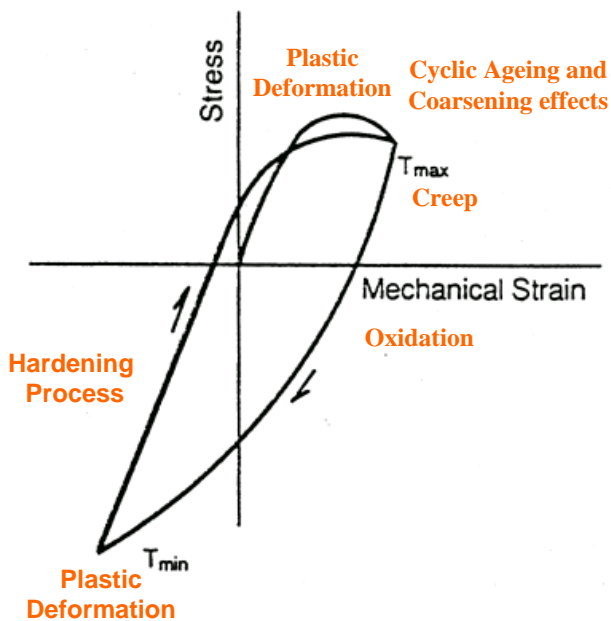
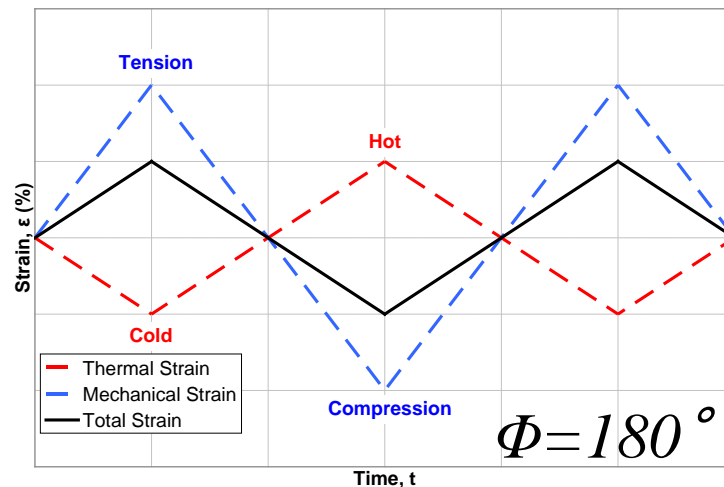
Virgin CMSX-8 monotonic response in the <111> dir



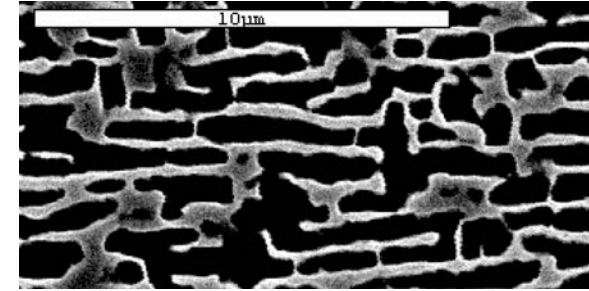
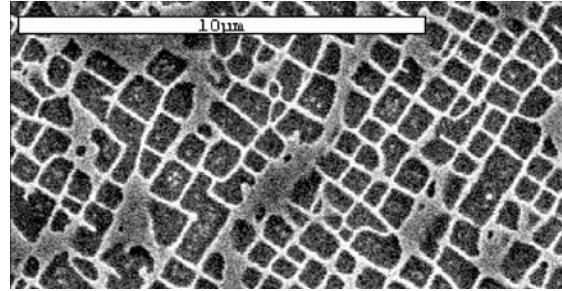
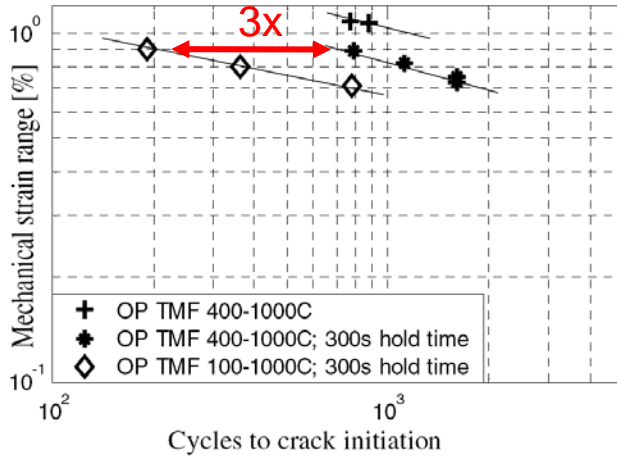
Linear In-Phase (IP)



Linear Out-of-Phase (OP)

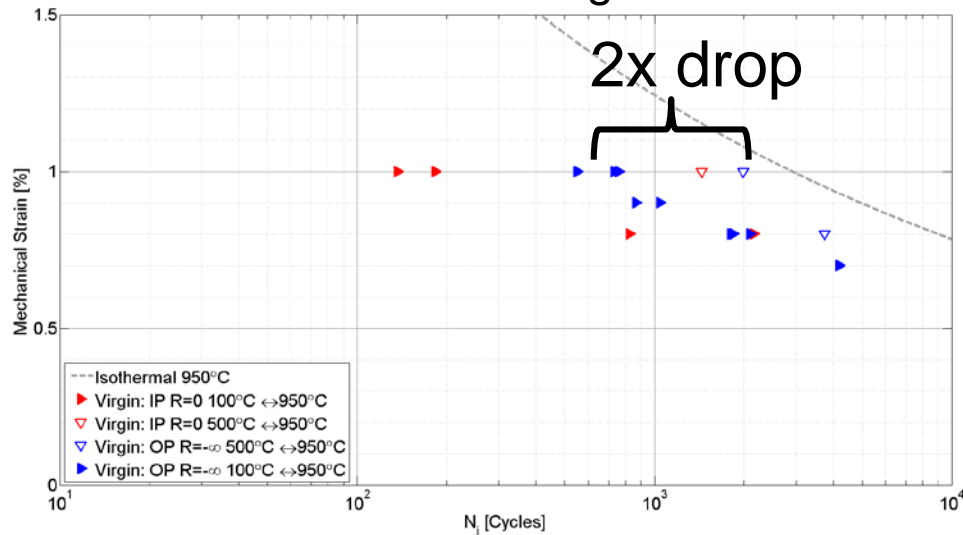


CMSX-4 [001]

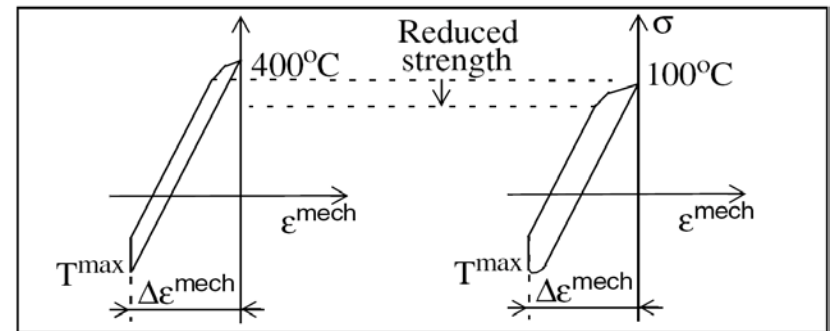


[Arrell et al., 2004]

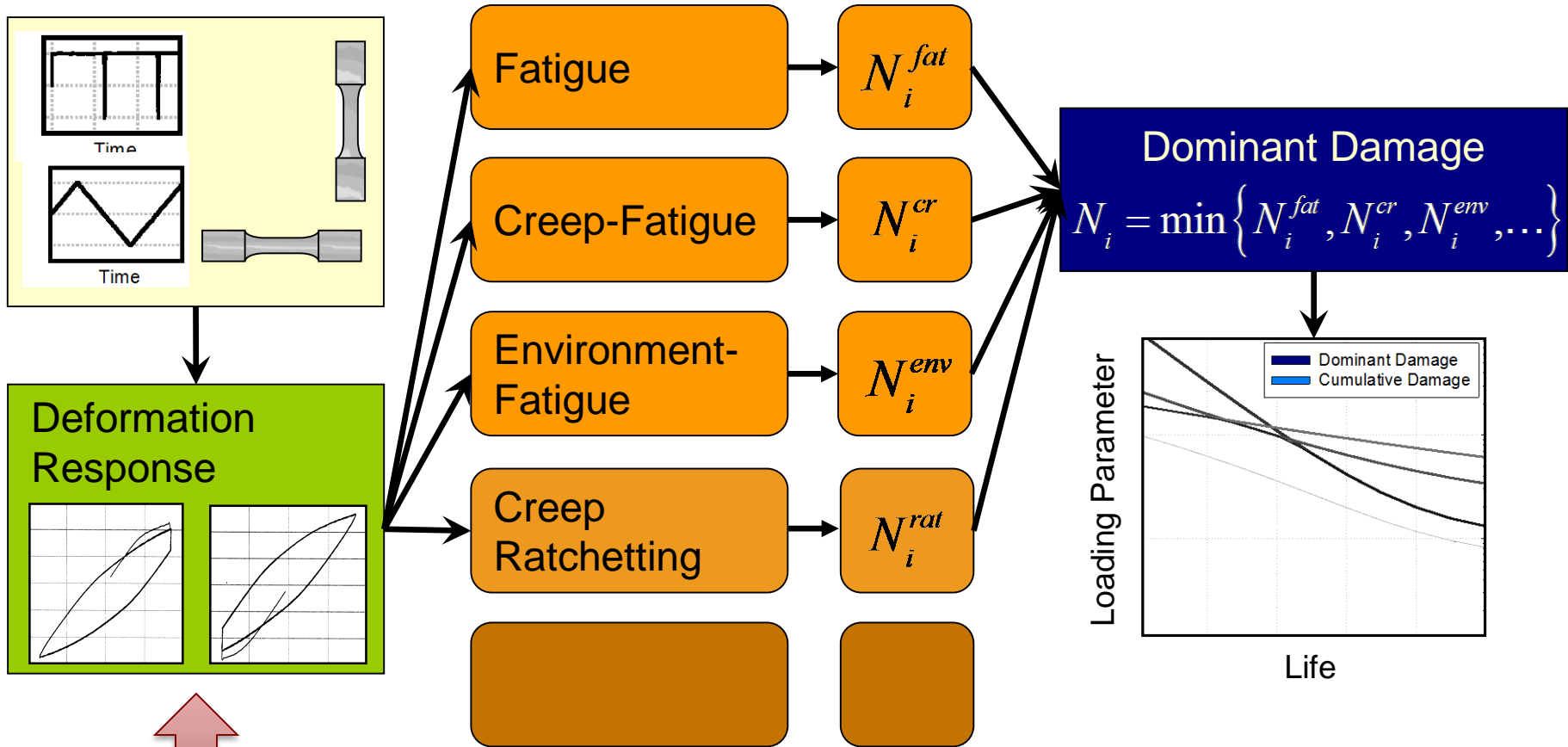
CM247LC DS in Longitudinal Dir.



[Kirka, 2014]



Damage Mechanism Modules

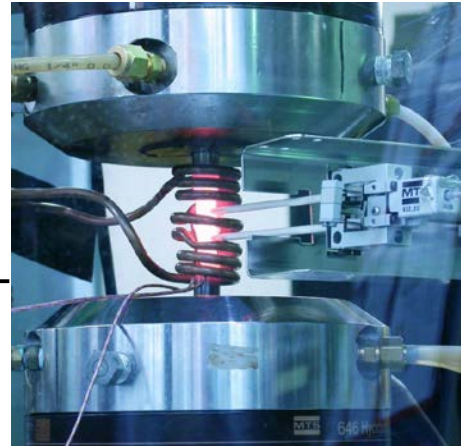


Accurate representations of the deformation response highly critical for predicting crack formation

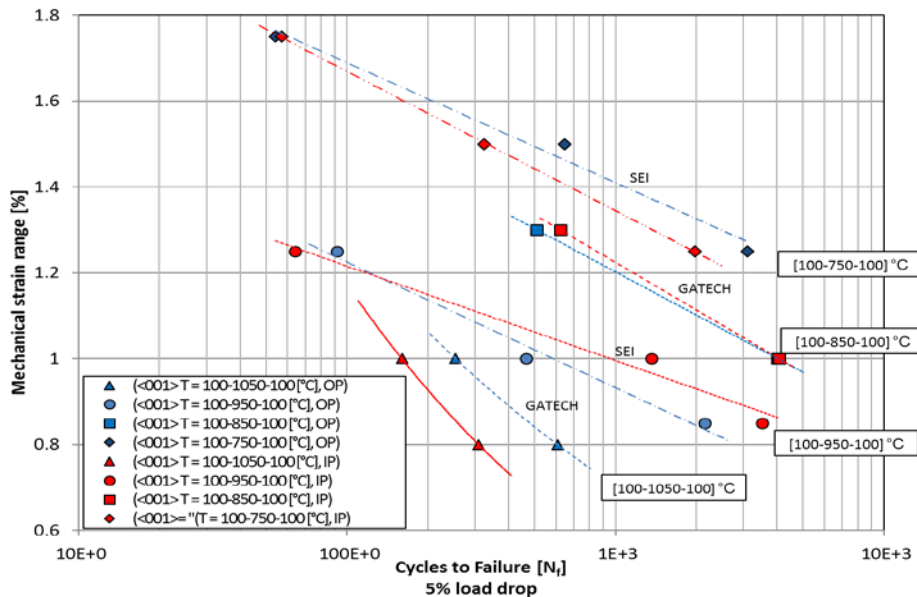
- Creep-fatigue interaction experiments on CMSX-8
- Influence of aging on microstructure and creep-fatigue interactions
- Microstructure-sensitive, temperature-dependent crystal viscoplasticity to capture the creep and cyclic deformation response

Experimentally establish the creep-fatigue interactions in a single-crystal Ni-base superalloy that is being targeted for use in industrial gas turbines (CMSX-8)

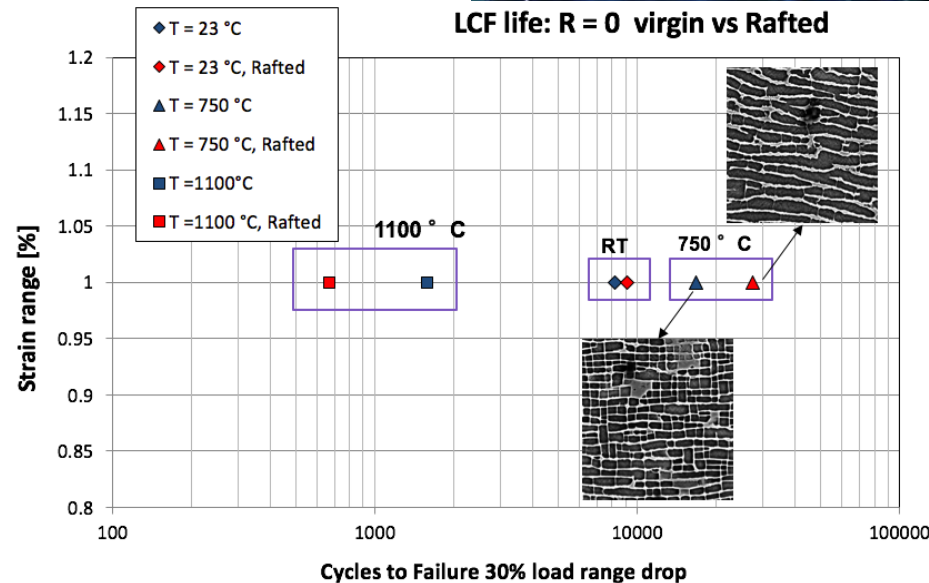
- Characterize creep-fatigue interactions on CMSX-8
 - Creep-fatigue
 - Thermomechanical fatigue
 - Creep (either tension or compression) followed by fatigue
 - Fatigue followed by creep
- Characterize the influence of aging on microstructure and creep-fatigue interactions

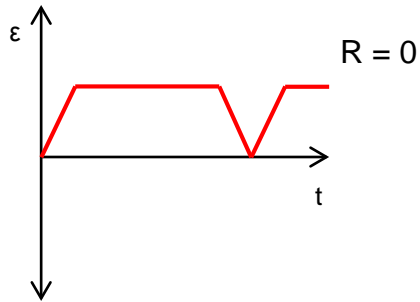


TMF life: In-Phase (R=0) vs Out-of-Phase (R=-inf)

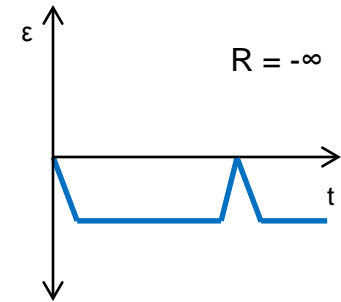
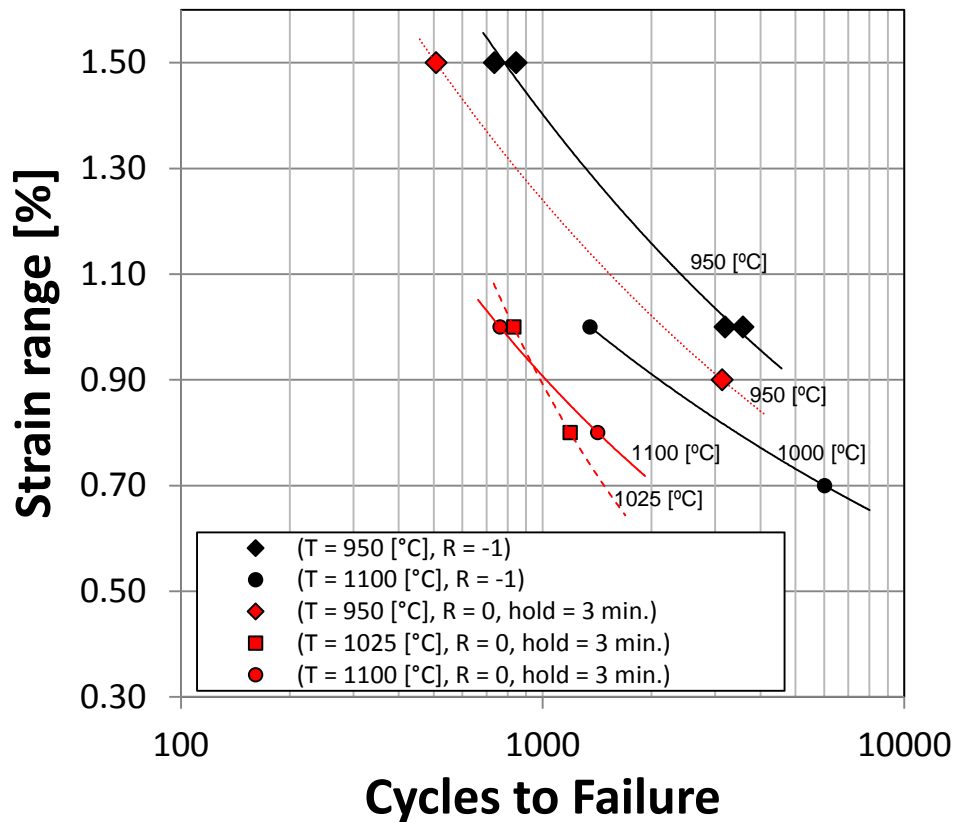


LCF life: R = 0 virgin vs Rafted

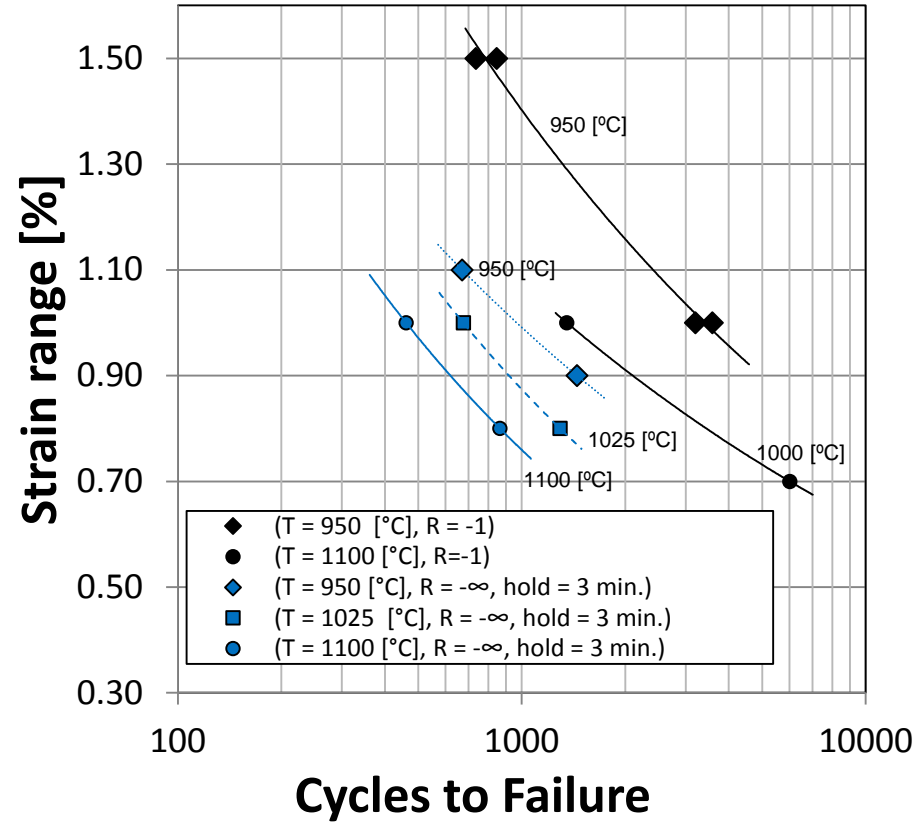


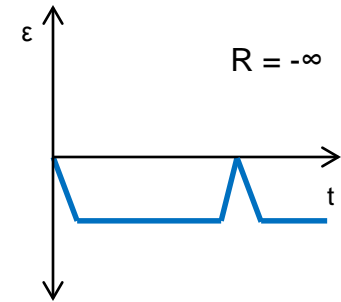
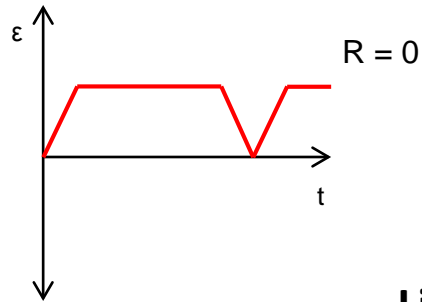


Effect of hold on LCF life: $R = 0$

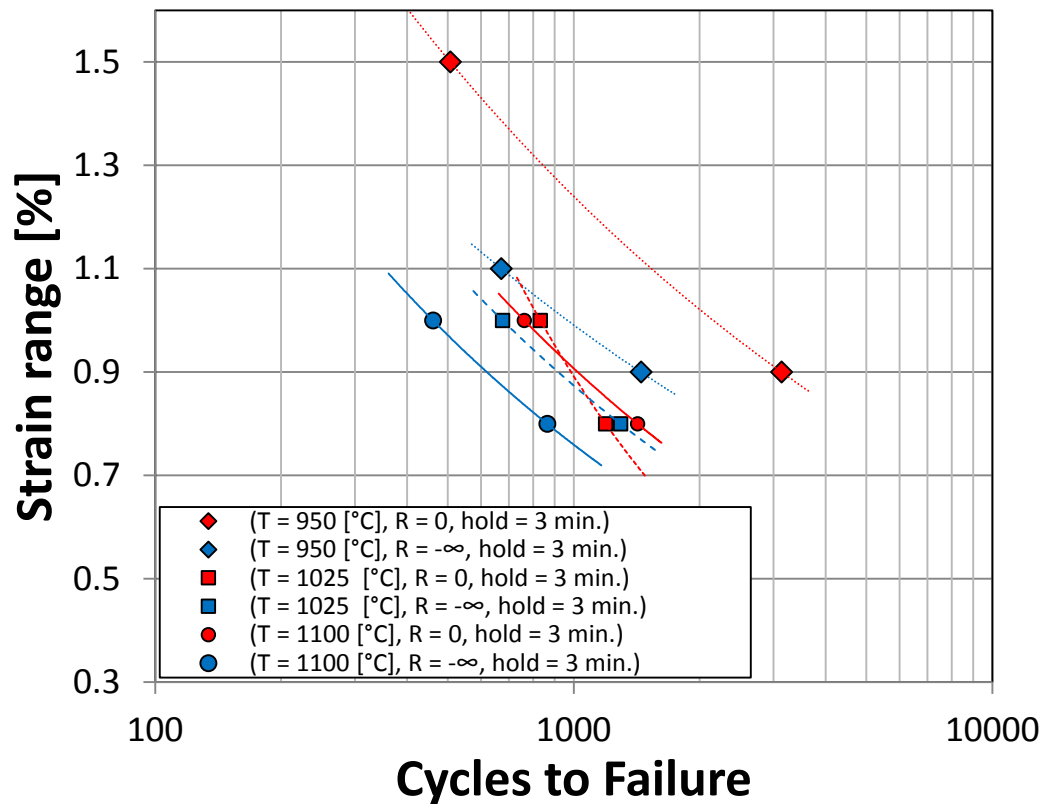


Effect of hold on LCF life: $R = -\infty$

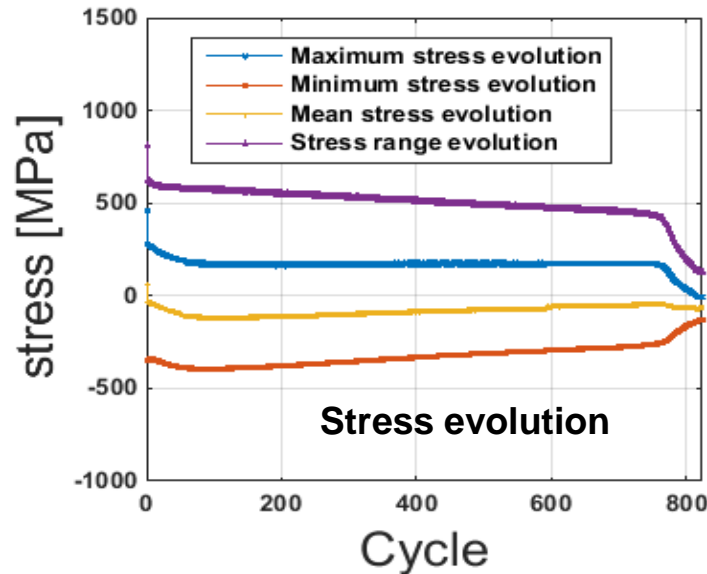
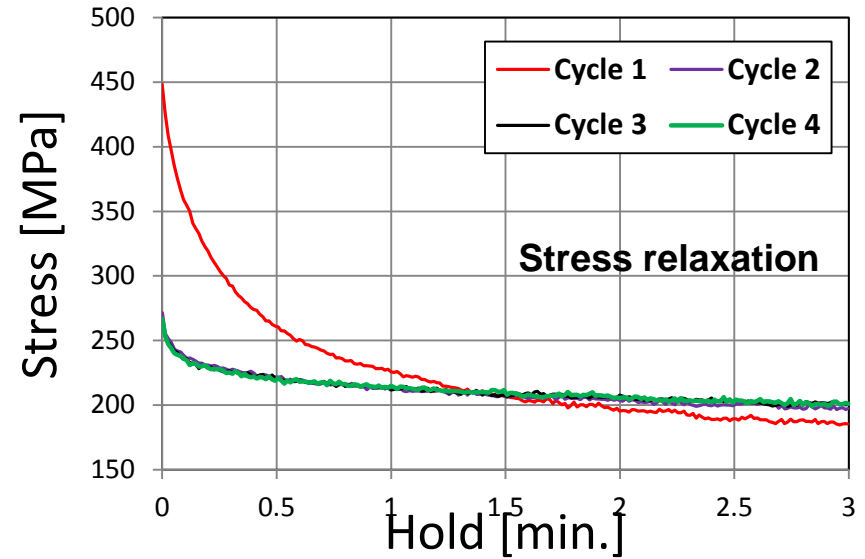
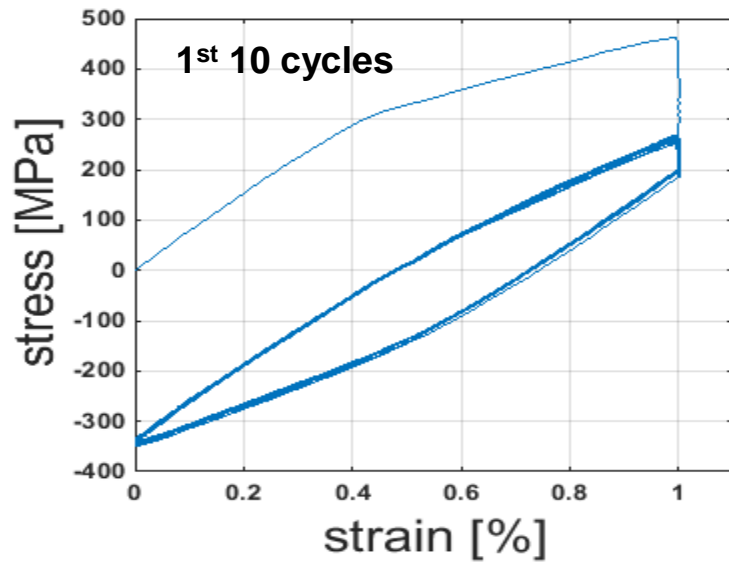




Life for low cycle creep-fatigue

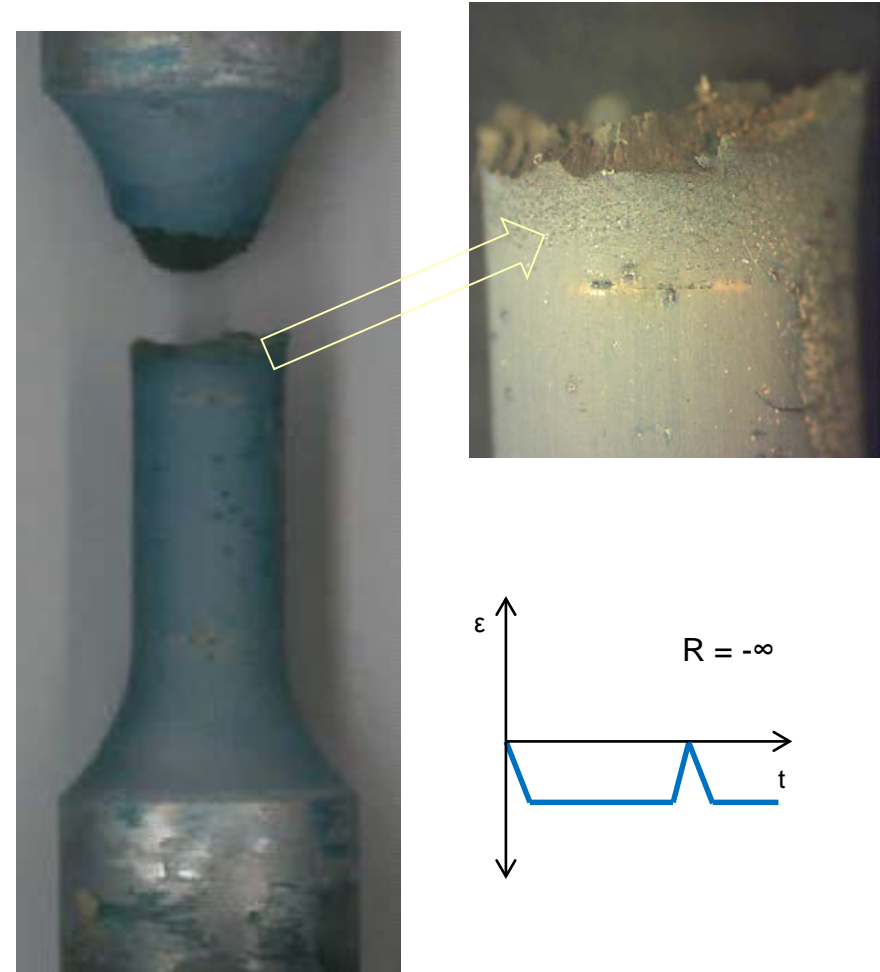
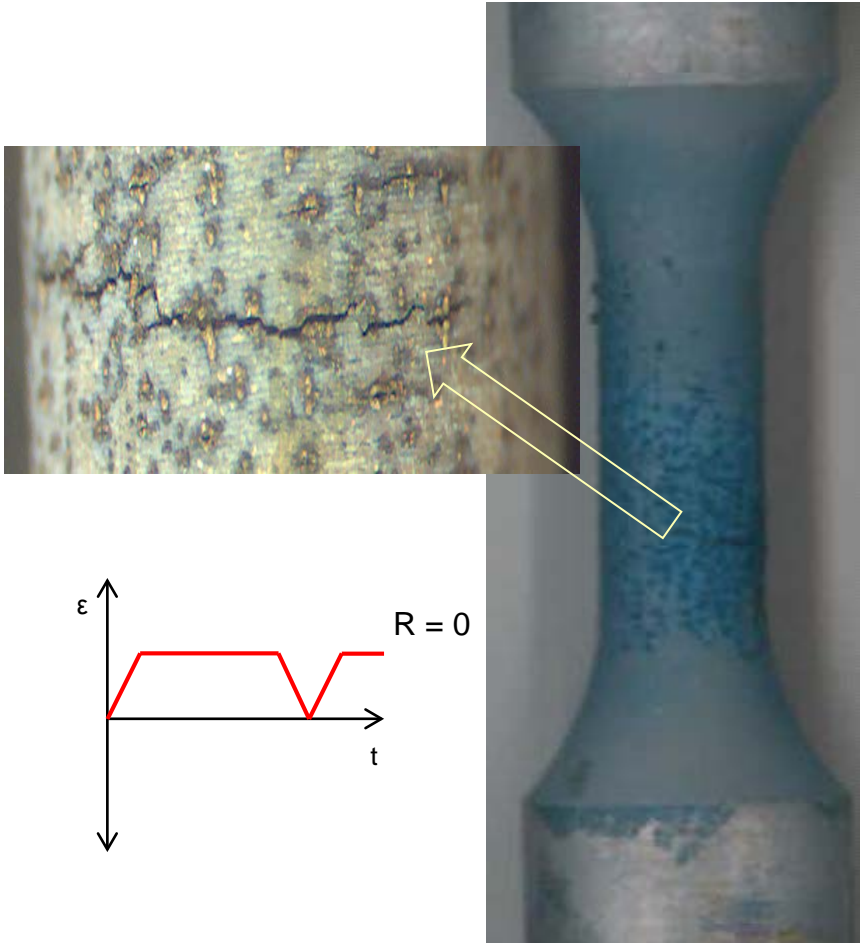


$T = 1100 \text{ }^\circ\text{C}$, $R = 0$, $\Delta\varepsilon = 1.0 \%$



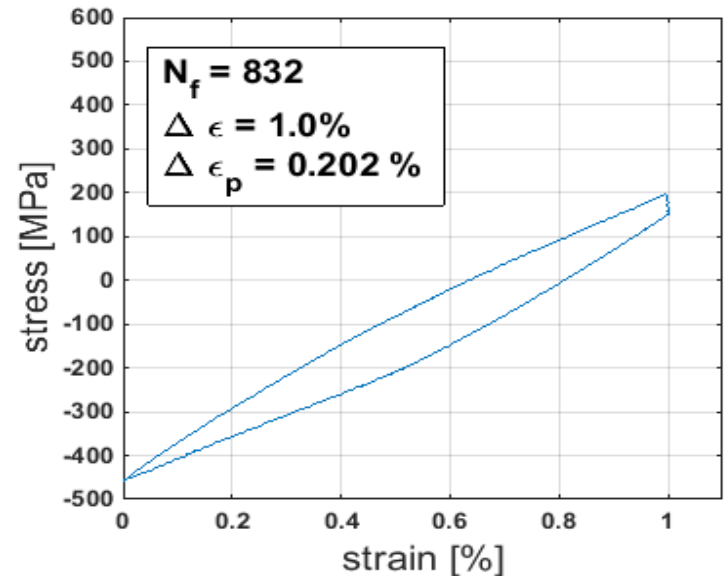
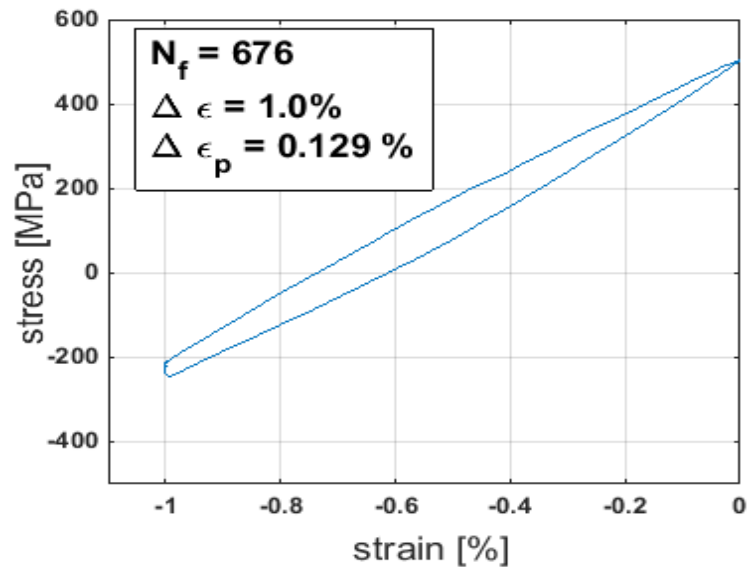
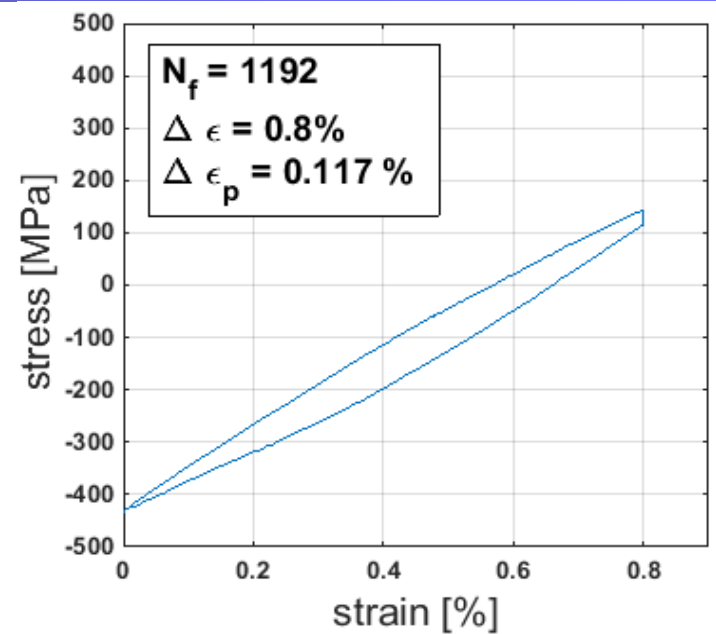
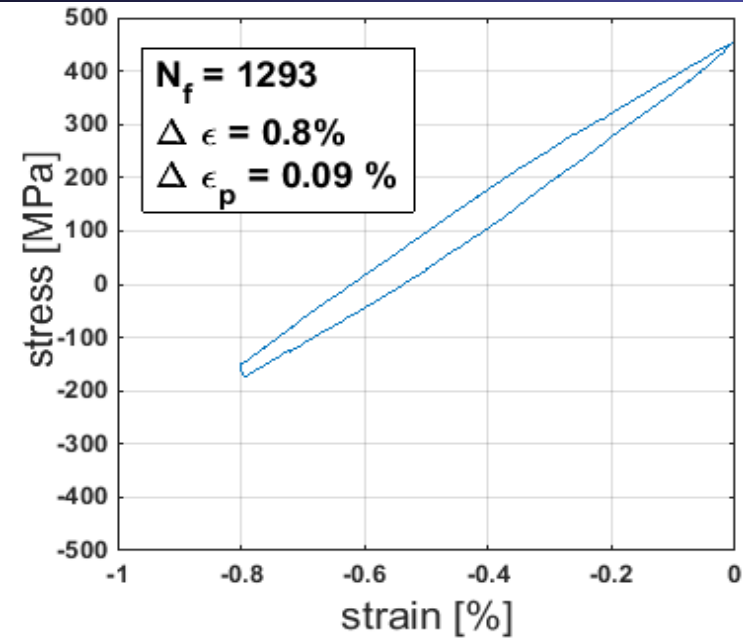
$R = 0, T = 1100^{\circ}\text{C}, \Delta\varepsilon = 0.8\%$
 $N_f = 1420$

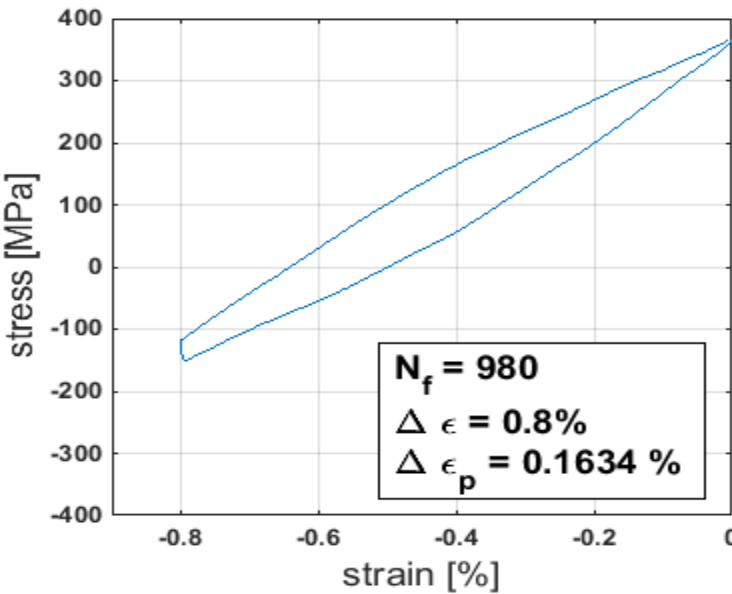
$R = -\infty, T = 1100^{\circ}\text{C}, \Delta\varepsilon = 0.8\%$
 $N_f = 980$



The George W. Woodruff School of Mechanical Engineering

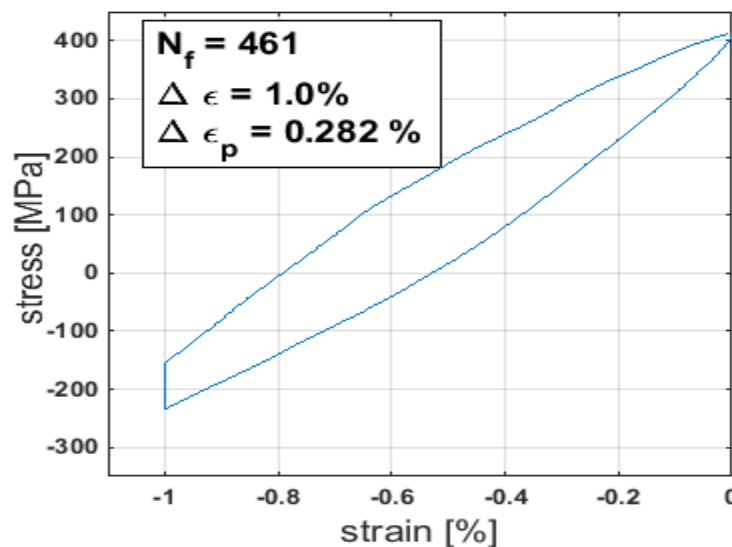
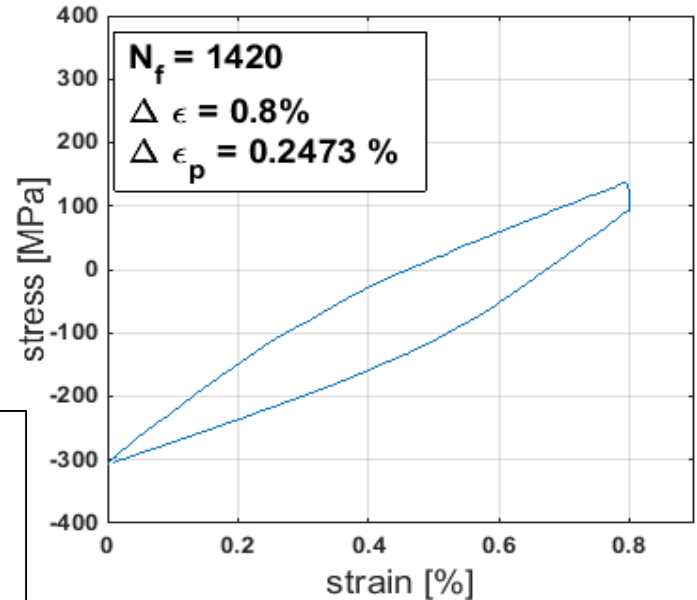
School of Materials Science and Engineering



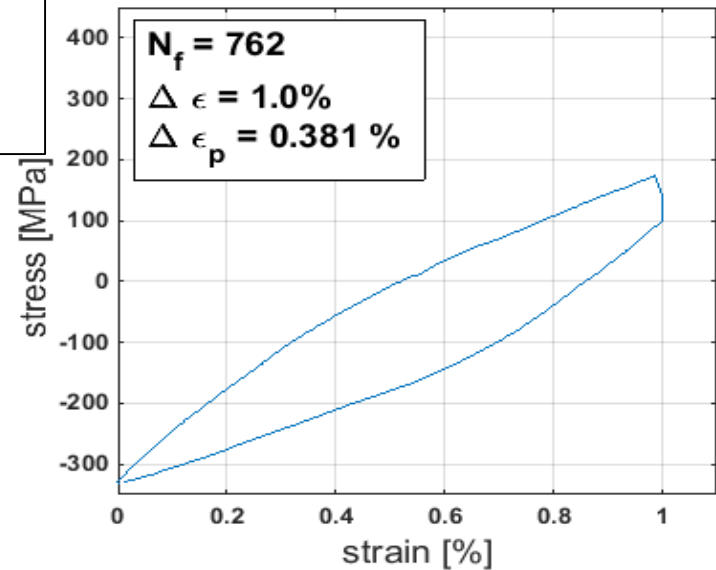


$\Delta \epsilon = 0.8 [\%]$

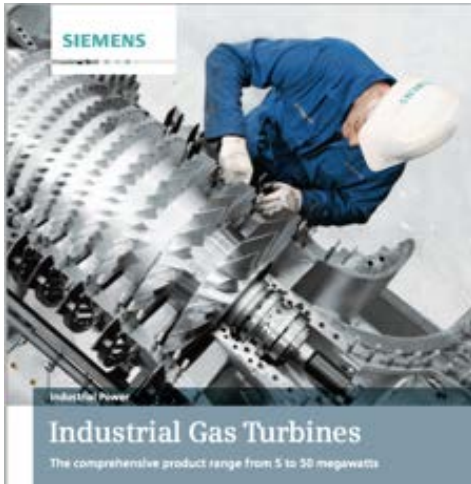
Plastic strain range alone does not explain life data at high temperatures. A Coffin-Manson relations would not be sufficient



$\Delta \epsilon = 1.0 [\%]$



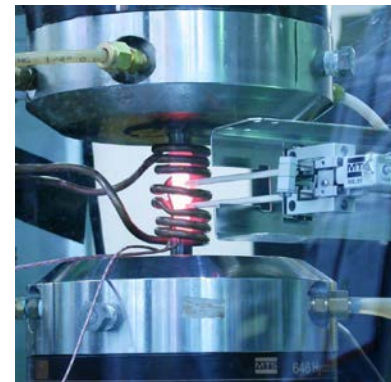
- Creep-fatigue interaction experiments on CMSX-8
- Influence of aging on microstructure and creep-fatigue interactions
- Microstructure-sensitive, temperature-dependent crystal viscoplasticity to capture the creep and cyclic deformation response



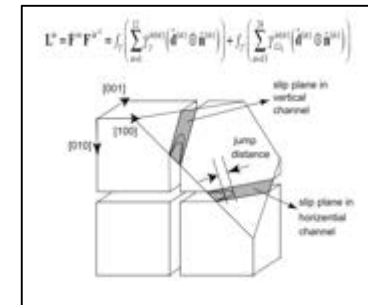
Microstructure-sensitive Crystal Viscoplasticity (CVP) Model to Determine Service “Process”-Structure-Property Linkages

$$\mathbf{L}^{in} = \dot{\mathbf{F}}^{in} \mathbf{F}^{in-1} = f_{\gamma} \left(\sum_{\alpha=1}^{12} \dot{\gamma}_{\gamma}^{in(\alpha)} (\hat{\mathbf{d}}^{(\alpha)} \otimes \hat{\mathbf{n}}^{(\alpha)}) \right) + f_{\gamma'} \left(\sum_{\alpha=13}^{24} \dot{\gamma}_{L12}^{in(\alpha)} (\hat{\mathbf{d}}^{(\alpha)} \otimes \hat{\mathbf{n}}^{(\alpha)}) \right)$$

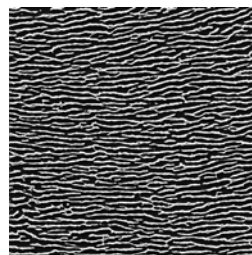
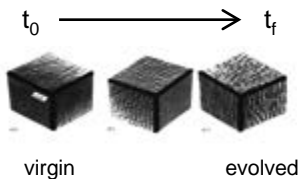
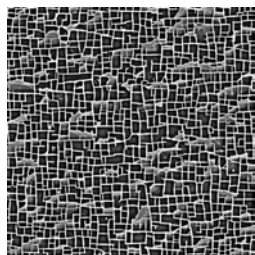
γ deformation



γ' deformation

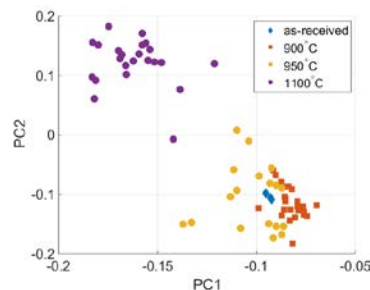


Experiments & Models to Predict Current State of Microstructure (Service Process-Structure Linkages)



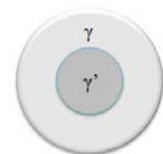
Sensitivity of Local Composition on Diffusivity for Input in Aging and Viscoplasticity Models

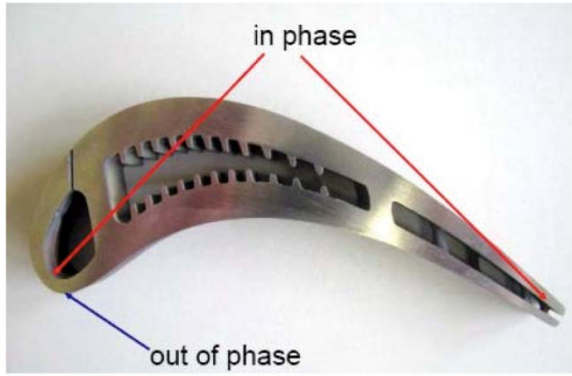
- Stress-free and stress-assisted (rafting) aging experiments under tensile and compressive stresses
- Establishing process-structure linkages using physical models, 2-point statistics and PCA



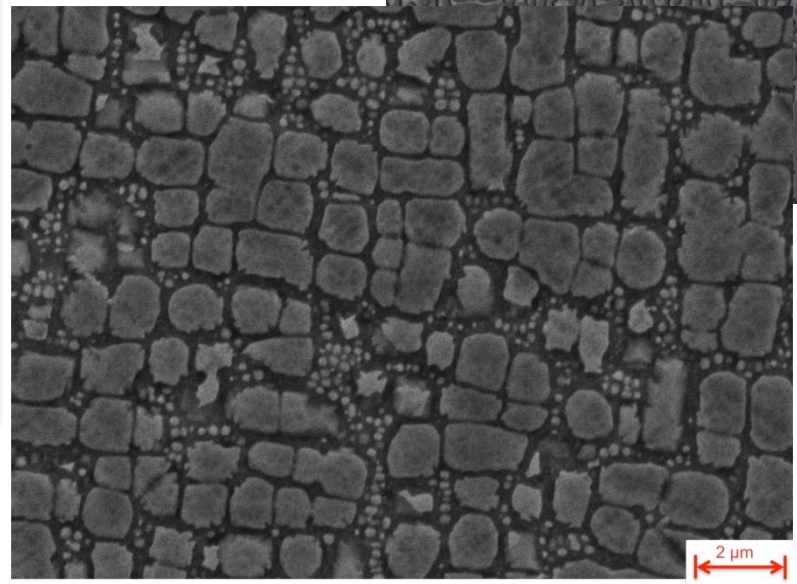
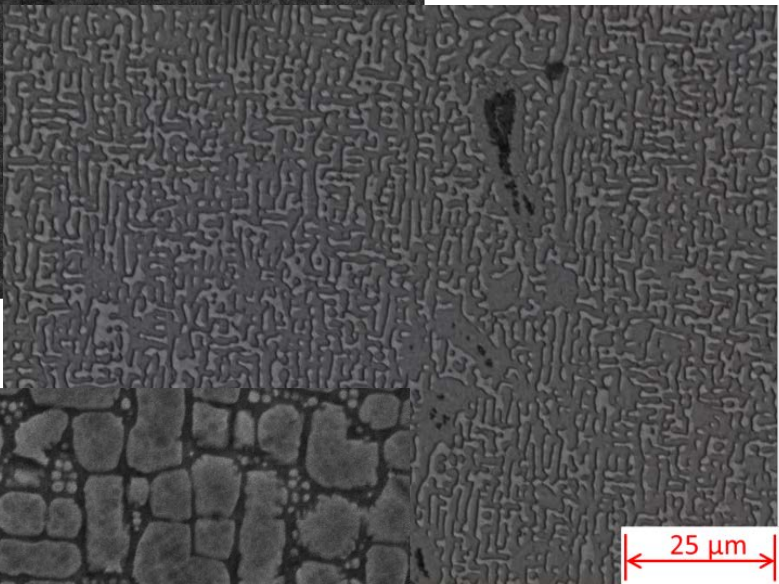
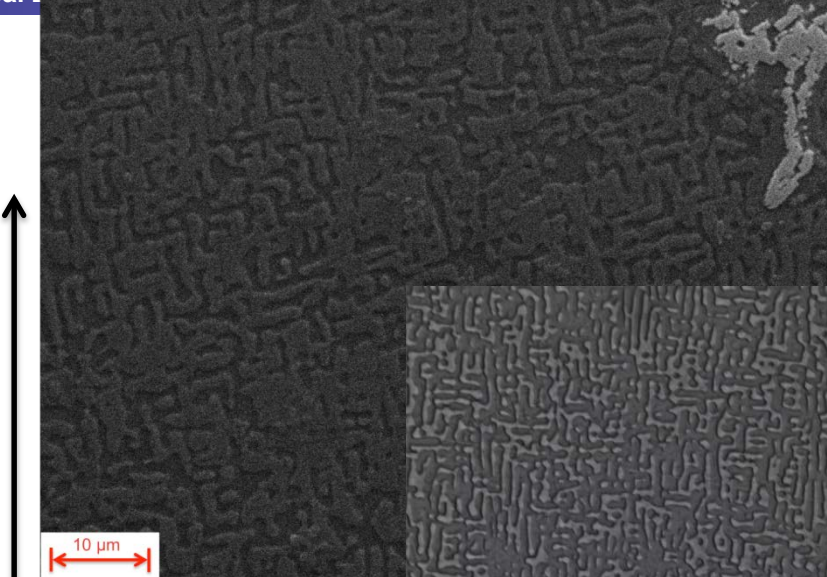
Thermo-Calc
DICTRA
Databases: TCNi5 / MOBNI2

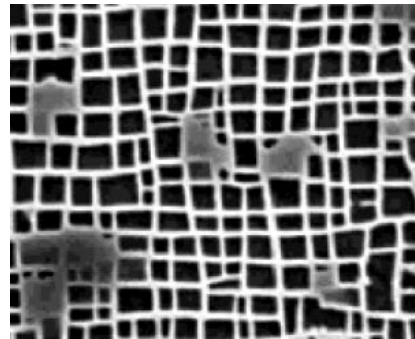
- Composition segregation in γ and γ' phase
- Determination of composition sensitive effective diffusivity to characterize aging activation energy and diffusivity parameter in viscoplasticity models





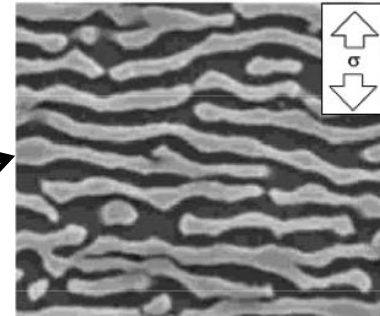
Distance from Root



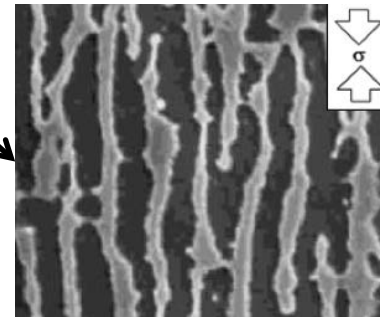


Tension

Compression

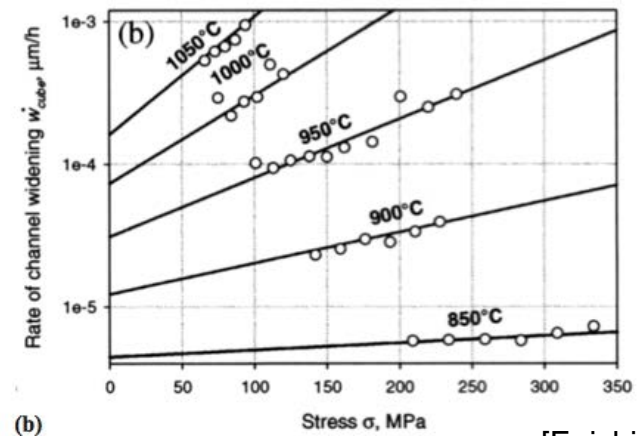
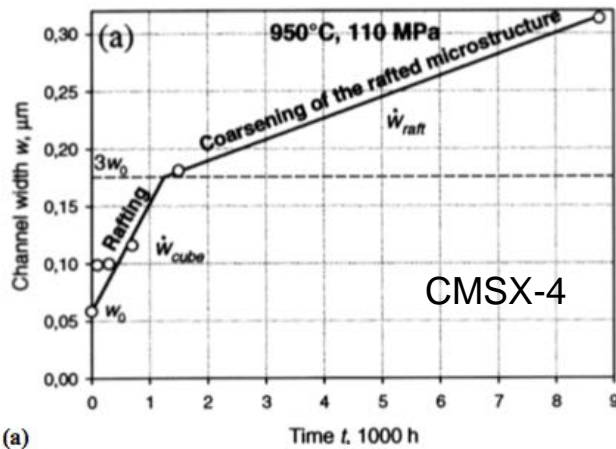


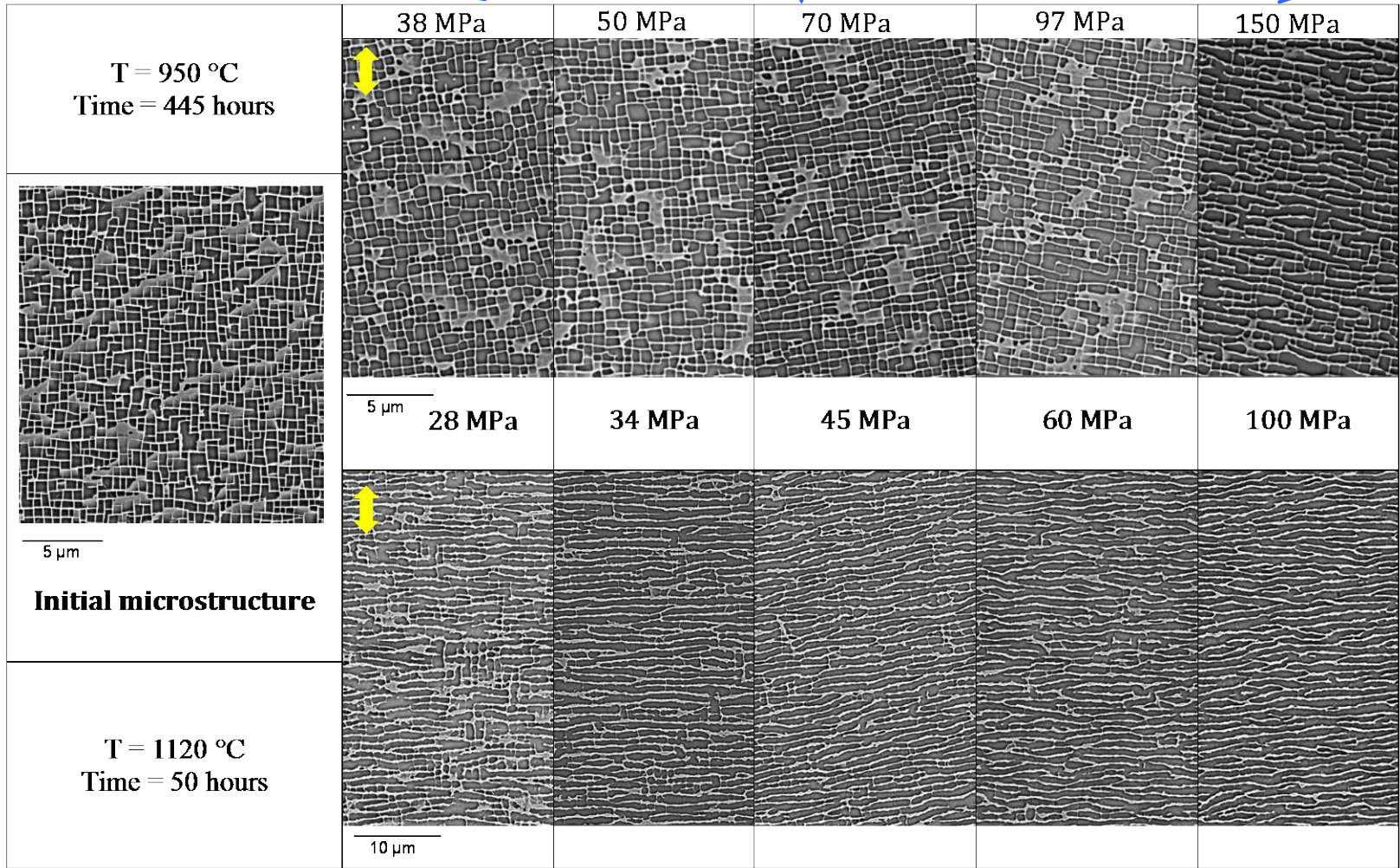
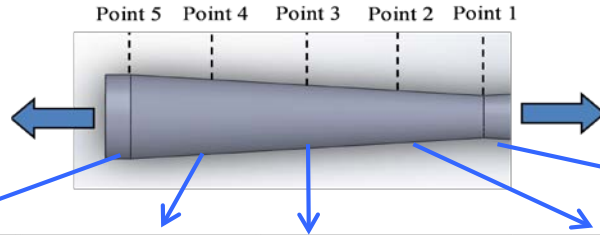
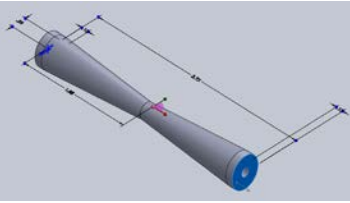
N-raft



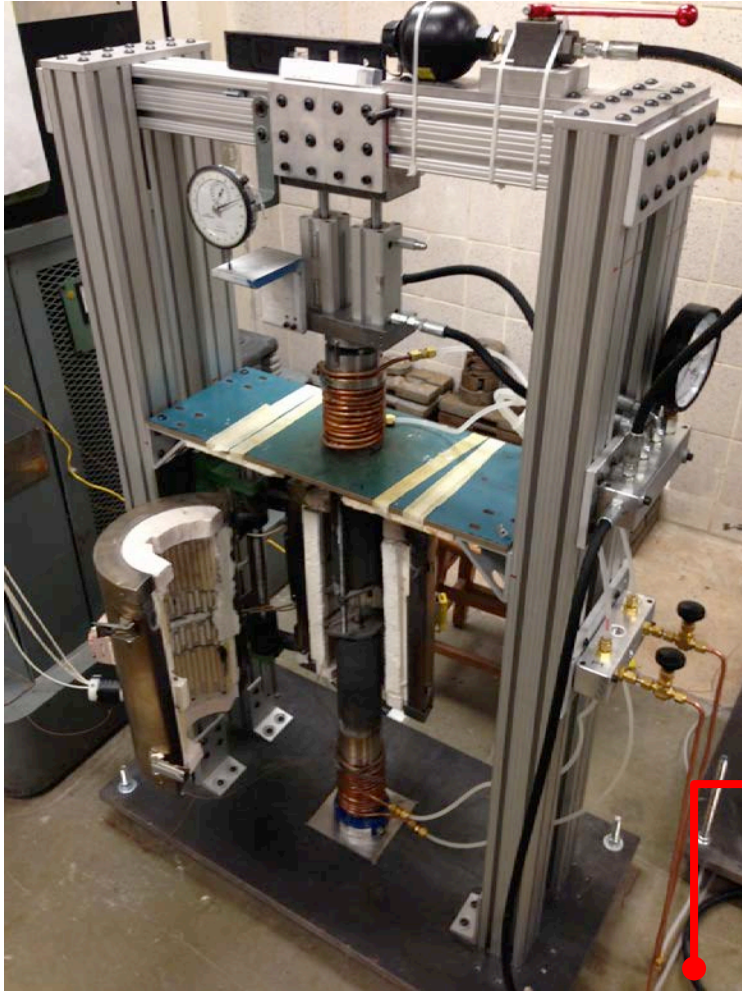
P-raft

$$\delta = \frac{2(a_{\gamma'} - a_{\gamma})}{a_{\gamma'} + a_{\gamma}}$$

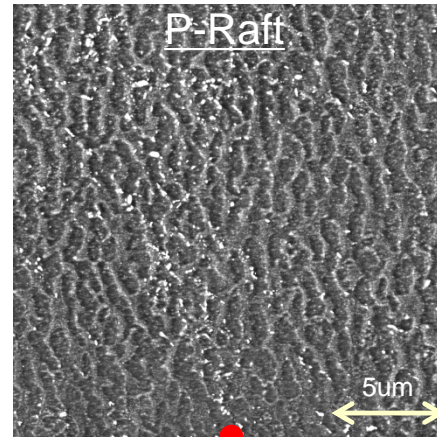




Compression Creep Frame

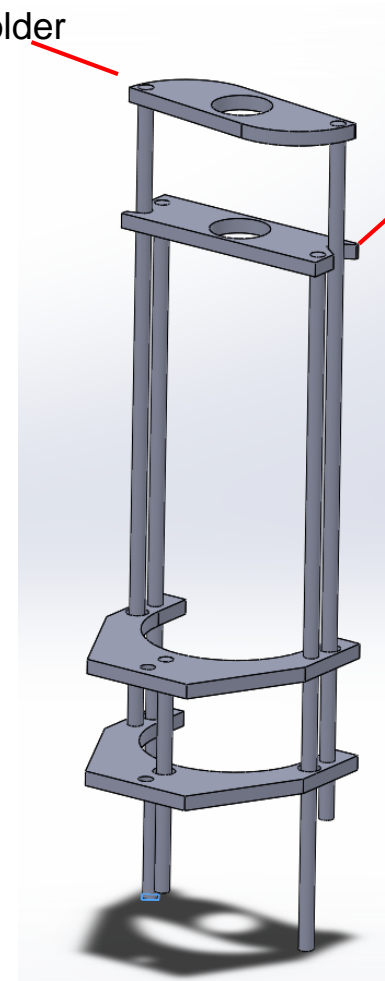


Ceramic Compression Creep Extensometer



Top Holder

Bottom Holder



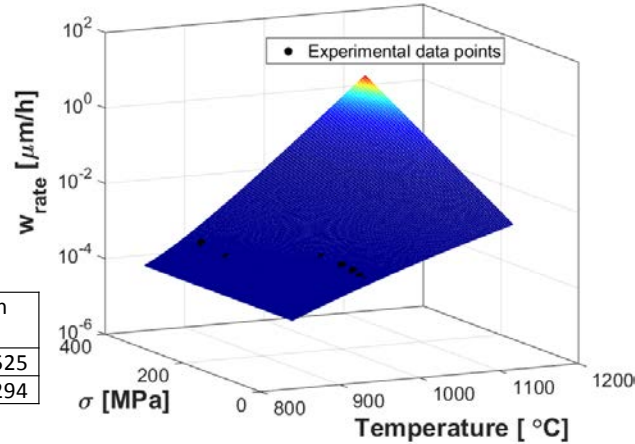
Physical aging models

Rafting

$$\dot{w}(T, \sigma) = A \cdot \exp\left[-\frac{Q - U(T) \cdot \sigma}{RT}\right]$$

$$U(T) = U_T(T - T_0)^n$$

	A ($\mu\text{m}/\text{h}$)	Q (kJ/mol)	U_T (J/mol.MPa.K ⁿ)	n
CMSX-8	2.0×10^5	206	0.033	1.525
CMSX-4	9.31×10^4	222	0.19	1.294

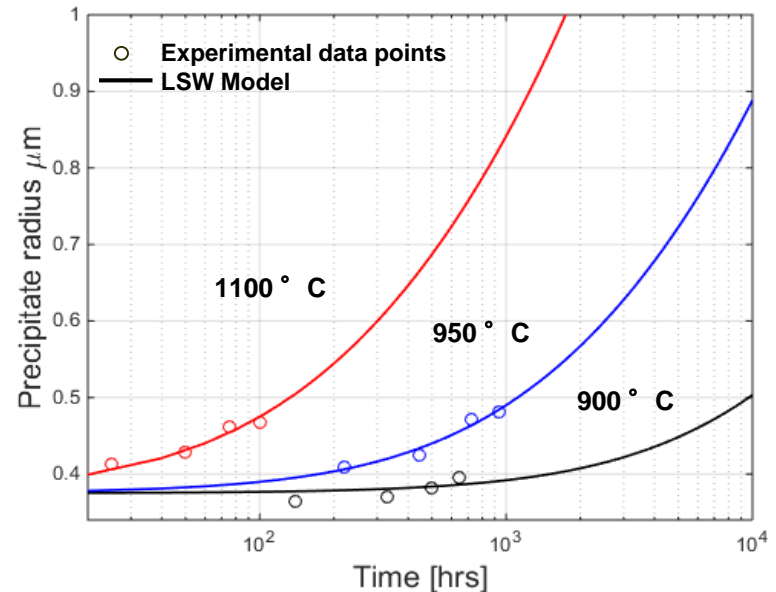
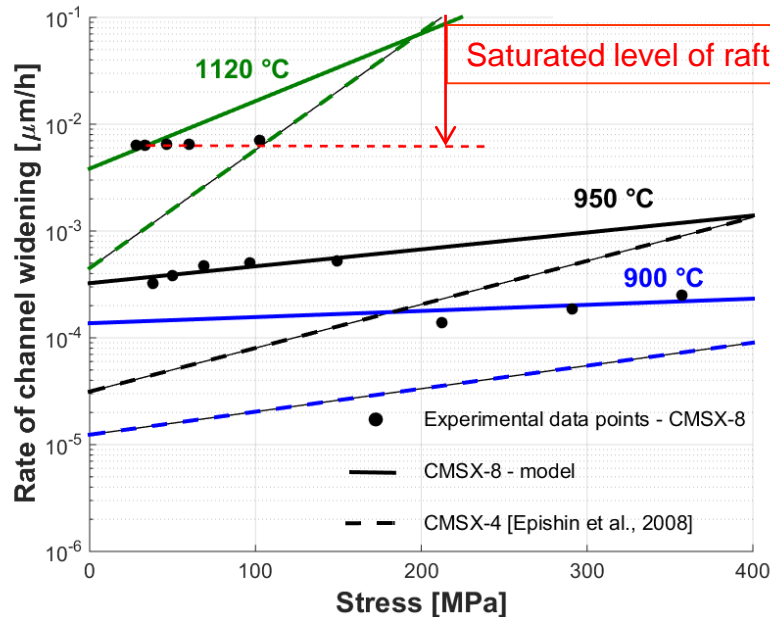


Coarsening

$$\text{LSW model: } (r)^3 - (r_0)^3 = Kt$$

$$K = K_0 \exp\left(-\frac{Q_{coar}}{RT}\right)$$

$$Q_{coar} (\text{CMSX} - 8) = 269.4 \text{ kJ/mol}$$



- 2-point correlation – A statistical representation of the microstructure that provides a magnitude measure in addition to the associated spatial correlation.

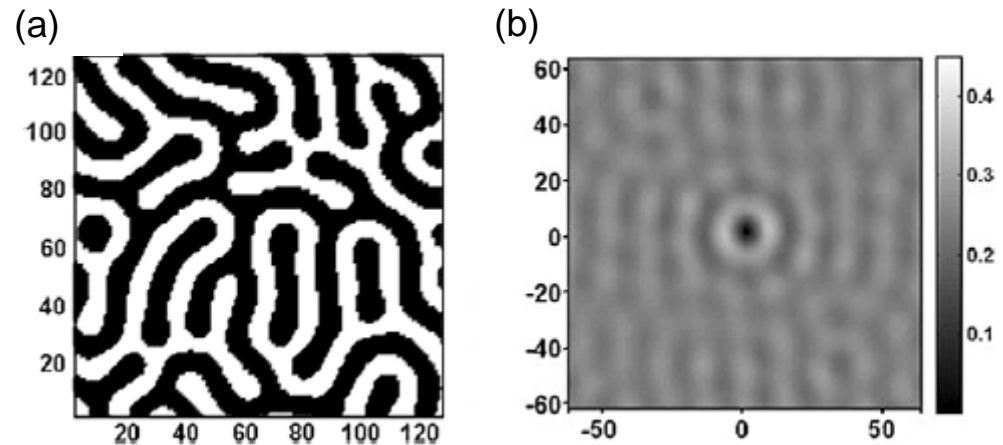
$$f(h, h' | \mathbf{r}) = \frac{1}{\text{vol}(\Omega)} \int_{\Omega} m(\mathbf{x}, h) m(\mathbf{x} + \mathbf{r}, h') d\mathbf{x}$$

$$\begin{aligned} {}^{np}F_{\mathbf{k}} &= \mathfrak{F}({}^{np}f_t) = \frac{1}{S} {}^nM_{\mathbf{k}}^* {}^pM_{\mathbf{k}} \\ &= \frac{1}{S} |{}^nM_{\mathbf{k}}| |{}^pM_{\mathbf{k}}| e^{-i {}^n\theta_{\mathbf{k}}} e^{i {}^p\theta_{\mathbf{k}}} \end{aligned}$$

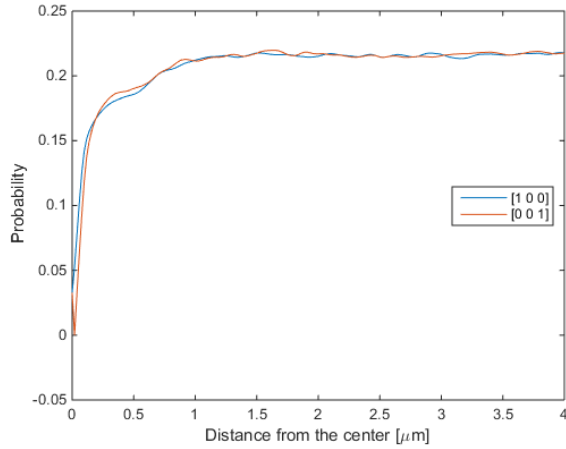
[Niezgoda, Fullwood and Kalidindi, 2008]

- 2-point correlations $f(h, h' | \mathbf{r})$ capture the probability density associated with finding an ordered pair of specific local state at the head and tail of a randomly placed vector \mathbf{r} into the microstructure.

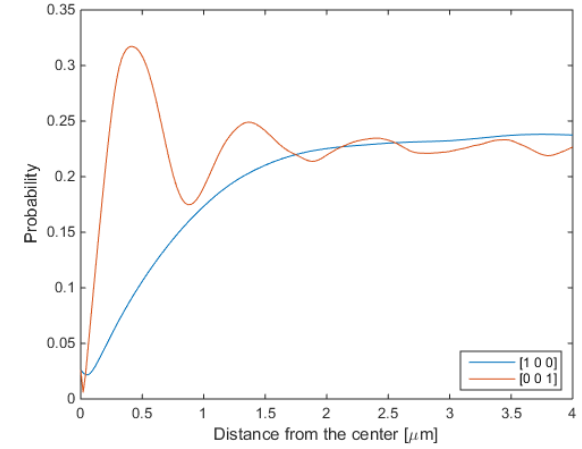
- **Cross-correlation**
Defined by $f(h, h' \neq h | \mathbf{r})$. The function gives the probability that a random vector of length x start in one phase and end in the other.



(a) An example of two phase microstructure (b) Cross-correlation for the black and white phases at the head and tail of a vector [Fullwood, Niezgoda, Adams, Kalidindi, 2010].

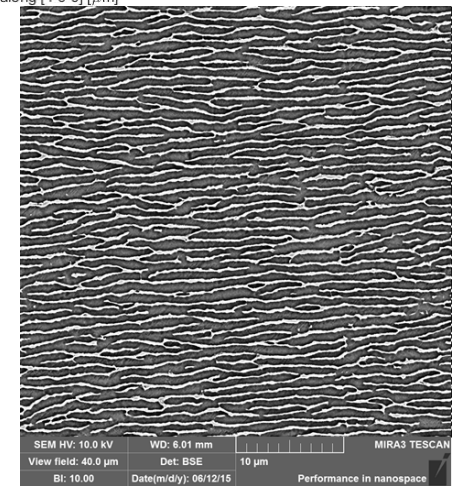
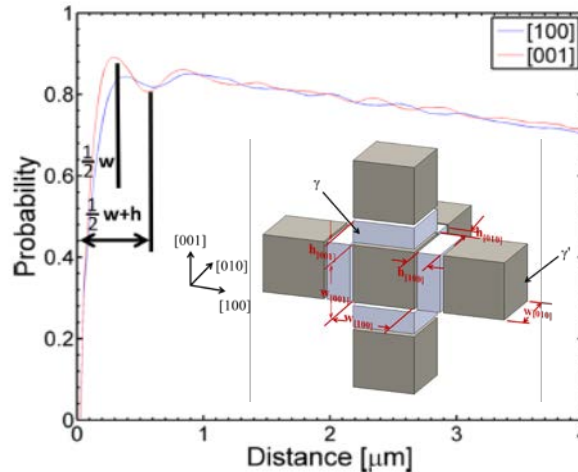
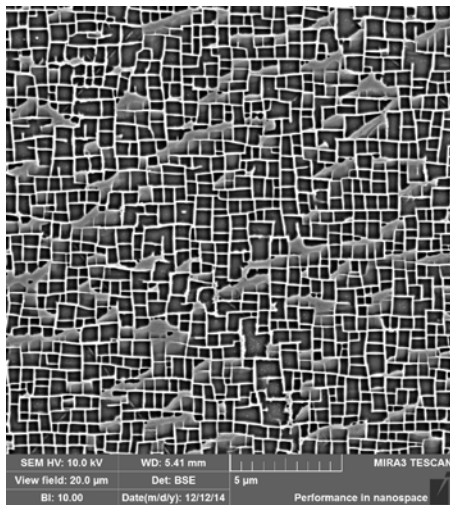
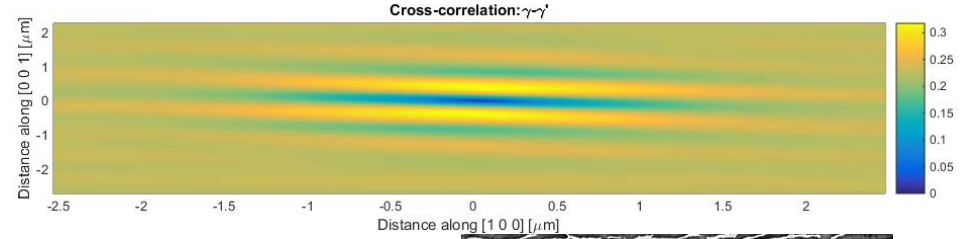
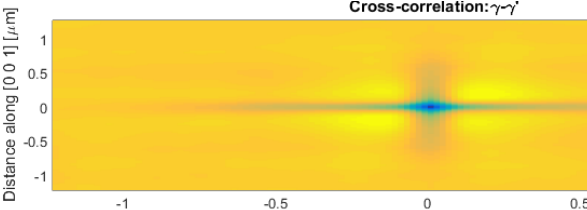


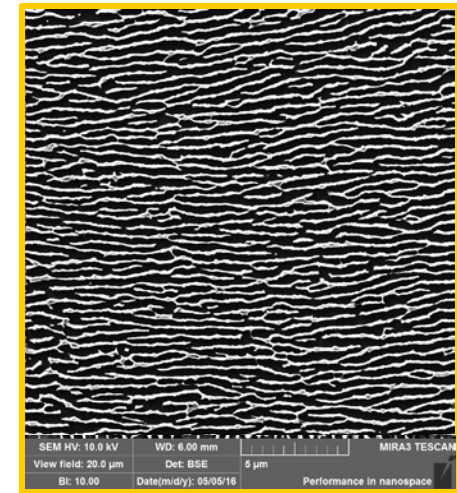
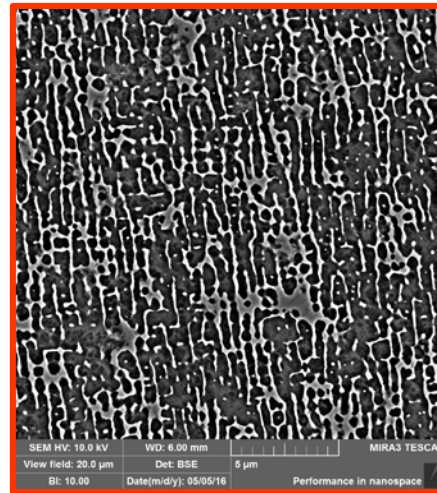
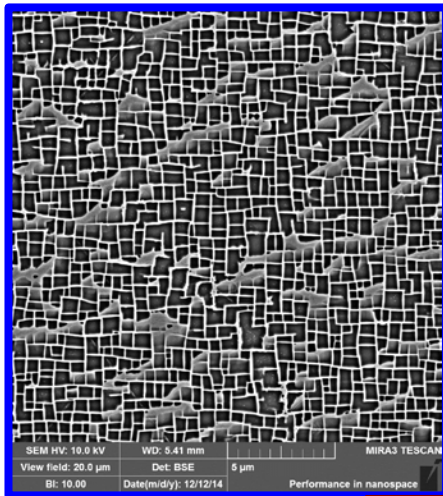
γ' precipitate and γ channel sizes are determined from the first peak and valley of the probabilistic curve of the corresponding micrograph.



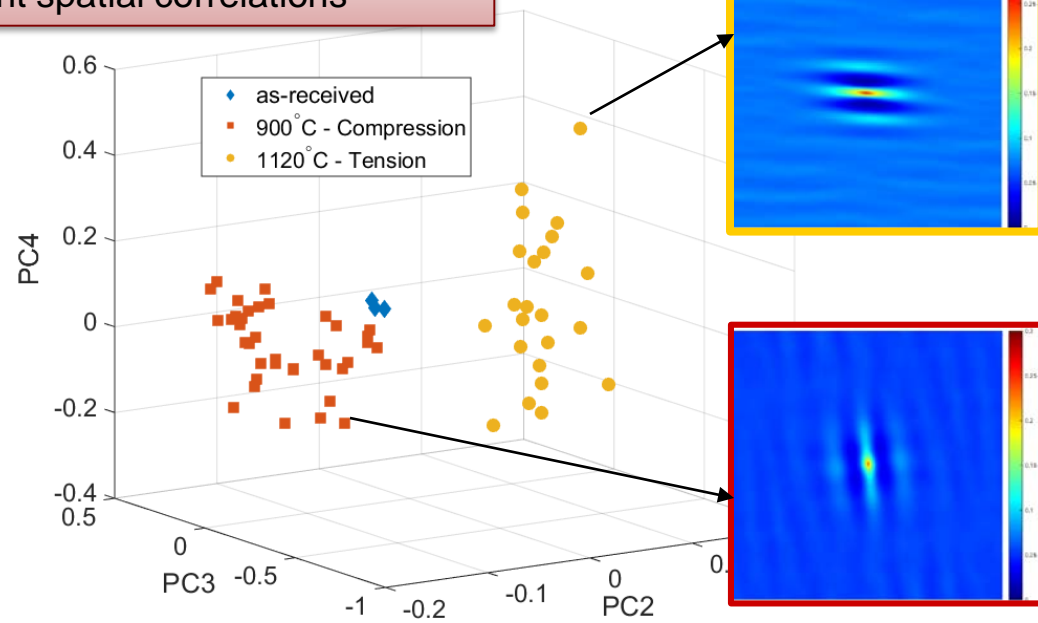
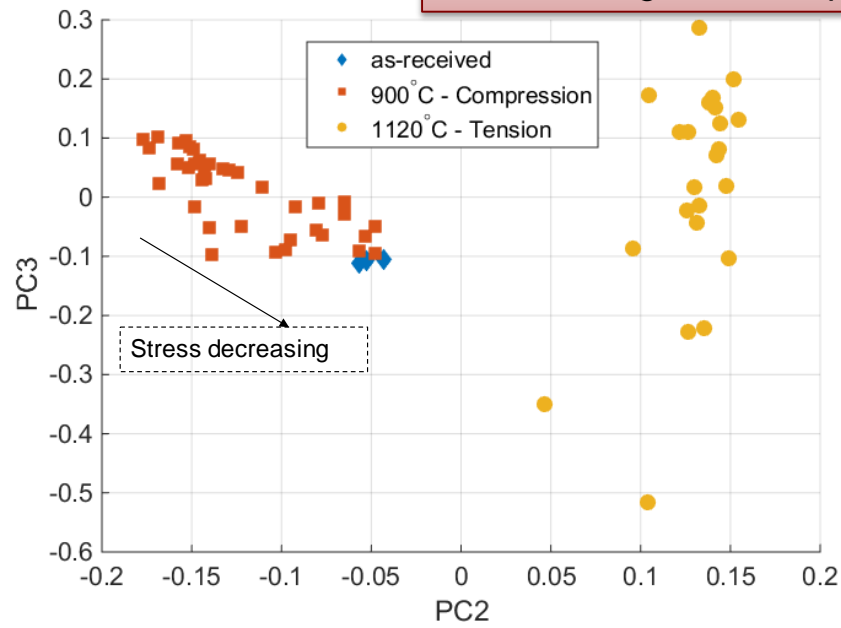
Cross-correlation: $\gamma-\gamma'$

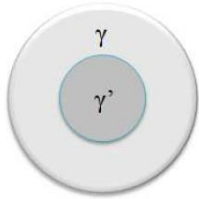
Cross-correlation: $\gamma-\gamma'$





Reduced order representation of aged microstructures using PCA of 2-point spatial correlations





Thermo-Calc DICTRA

Databases: TCNi5 / MOBNI2

Composition sensitive diffusivity parameter

Aging behavior

Temperature-dependent constitutive models

LSW model

$$r^3 - r_o^3 = K(t - t_o)$$

$$K = \frac{64D_{eff}C_{\infty}\sigma\Omega^2}{9RT}$$

$$D_{eff} = D_{0,eff} \left(-\frac{Q_{eff}}{RT} \right)$$

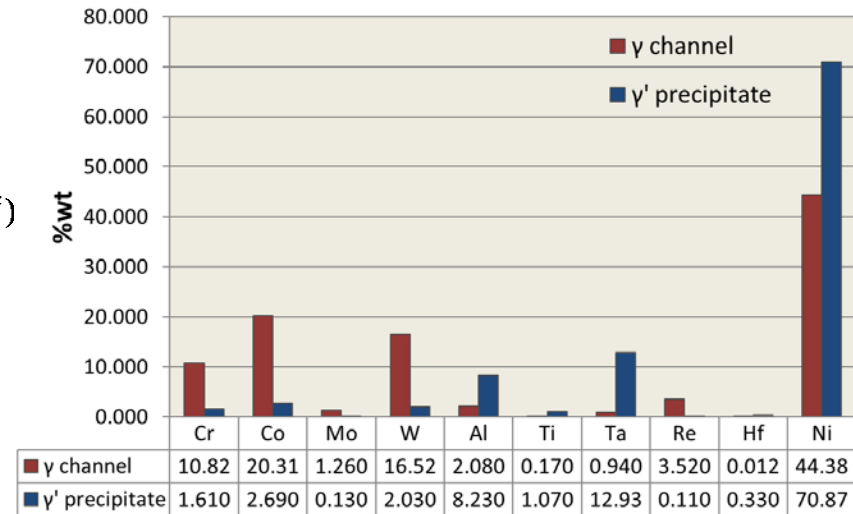
Coarsening effective diffusivity

$$\chi^{\alpha} = \chi_0^{\alpha} \Theta(T) \left\langle \frac{\tau_v^{\alpha}}{D^{\alpha}} \right\rangle^n \exp \left\{ B_0 \left\langle \frac{\tau_v^{\alpha}}{D^{\alpha}} \right\rangle^{n+1} \right\} \text{sgn}(\tau^{\alpha} - \chi^{\alpha})$$

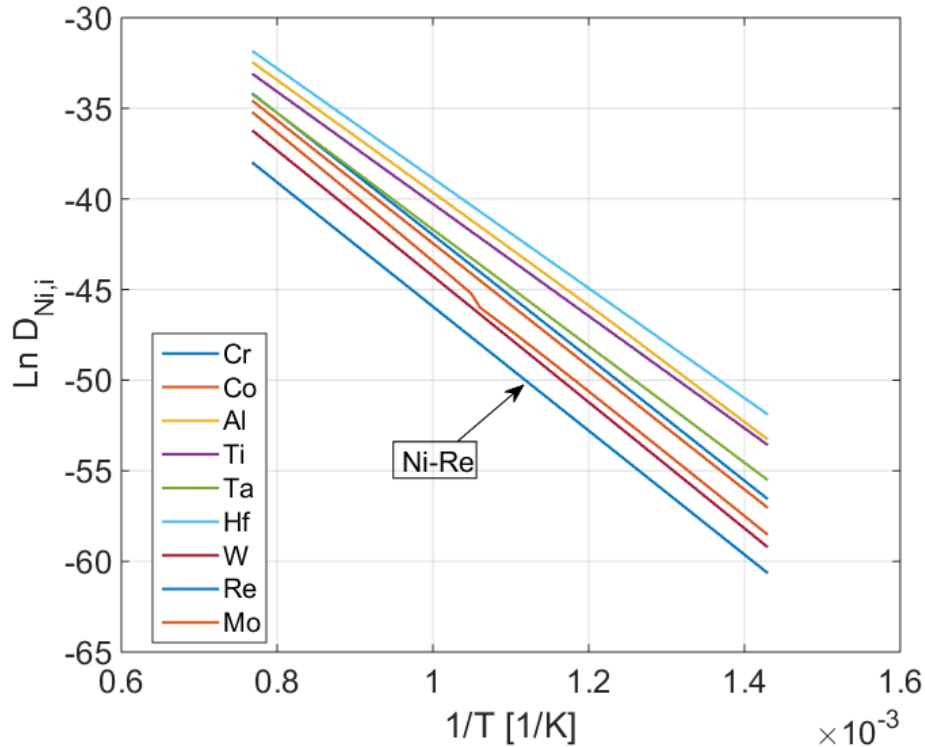
$$\Theta(T) = \exp\left(-\frac{Q_0}{RT}\right)$$

Diffusivity parameter

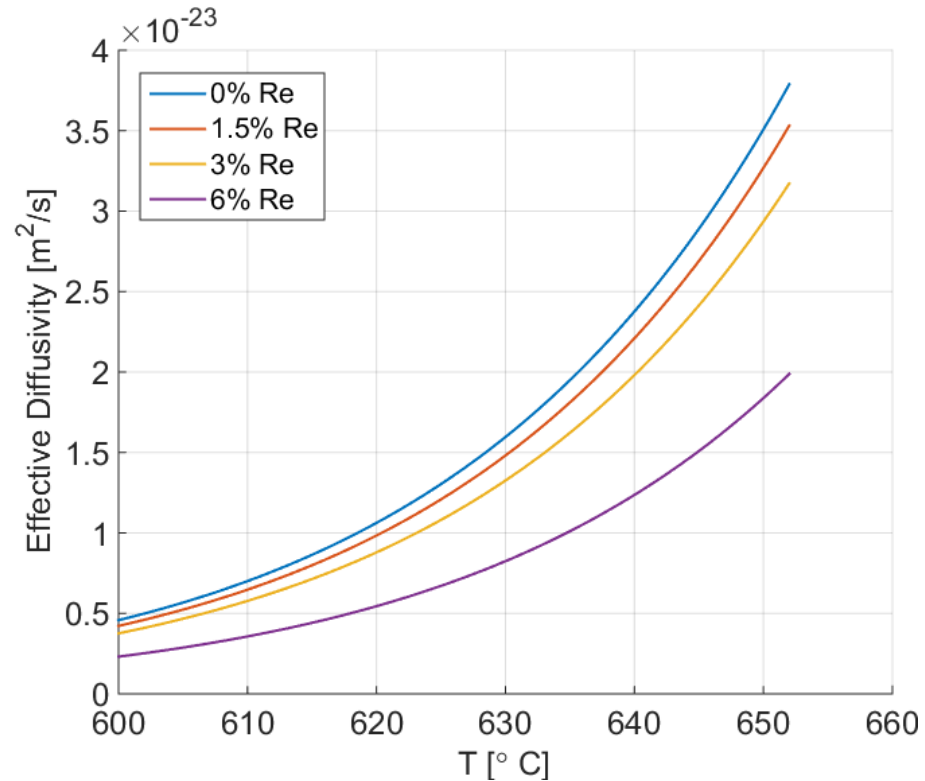
Composition segregation
Thermo-Calc



Interdiffusion coefficients of Ni-x binary systems
DICTRA



Composition variation (Re) effect on effective diffusivity of the complex Superalloy system
DICTRA



$$D_{Ni-x} = D_{0,Ni-x} \left(-\frac{Q_{Ni-x}}{RT} \right) \quad Q_{eff} = \sum_{i=1}^n x_x Q_{Ni-x}$$

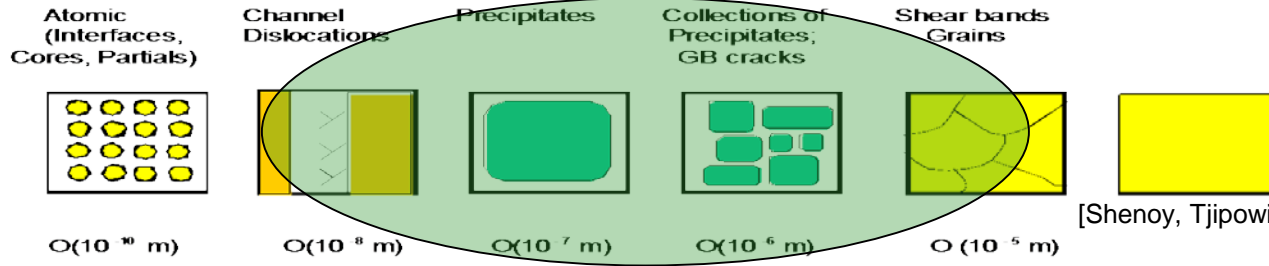
Molar fraction of element x

**Effective activation energy/
Coarsening activation energy**

= 275.9 KJ/mol

- Creep-fatigue interaction experiments on CMSX-8
- Influence of aging on microstructure and creep-fatigue interactions
- **Microstructure-sensitive, temperature-dependent crystal viscoplasticity to capture the creep and cyclic deformation response**

Alloy structure



[Sheny, Tjipowidjojo, and McDowell, 2008]

+

Distinct deformation in the γ and γ' phases

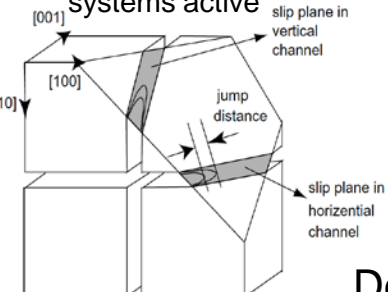
$$\mathbf{L}^{in} = f_{\gamma} \left(\sum_{\alpha=1}^{12} \dot{\gamma}_{\gamma}^{in(\alpha)} (\hat{\mathbf{d}}^{(\alpha)} \otimes \hat{\mathbf{n}}^{(\alpha)}) \right) + f_{\gamma'} \left(\sum_{\alpha=13}^{24} \dot{\gamma}_{L1_2}^{in(\alpha)} (\hat{\mathbf{d}}^{(\alpha)} \otimes \hat{\mathbf{n}}^{(\alpha)}) \right)$$

+

Deformation predictions sensitive to the γ and γ' phase attributes

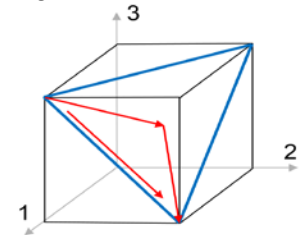
γ deformation

In γ : 12 octahedral slip systems active

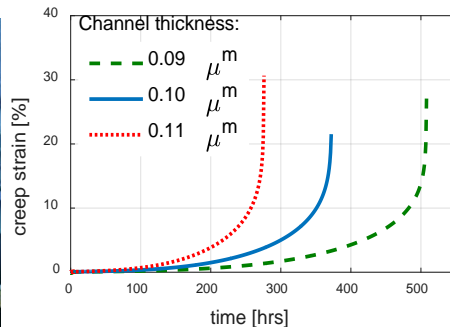
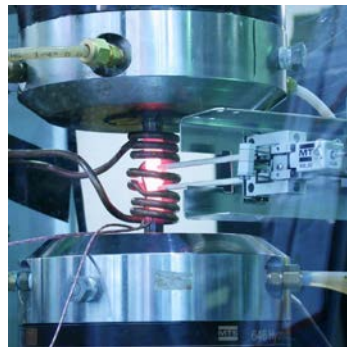


γ' deformation

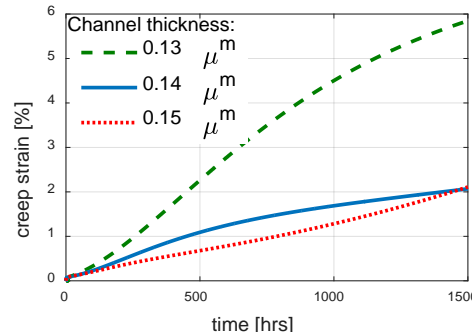
In γ' : 12 octahedral slip systems moving as dislocation ribbons



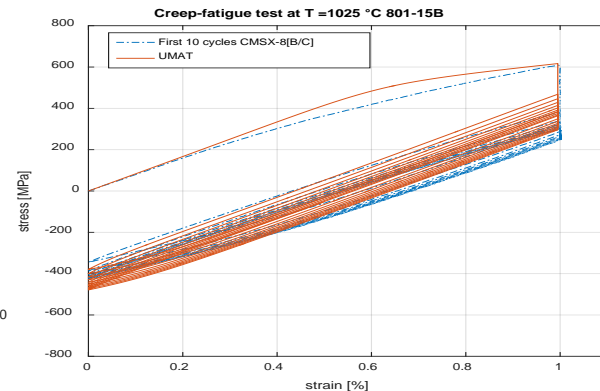
[Ma, Dye, and Reed, 2008]



Tertiary creep: 950 °C, Stress = 400 MPa



Primary creep: 750 °C, Stress = 680 MPa



Kinematic relations including temperature dependence

Deformation gradient

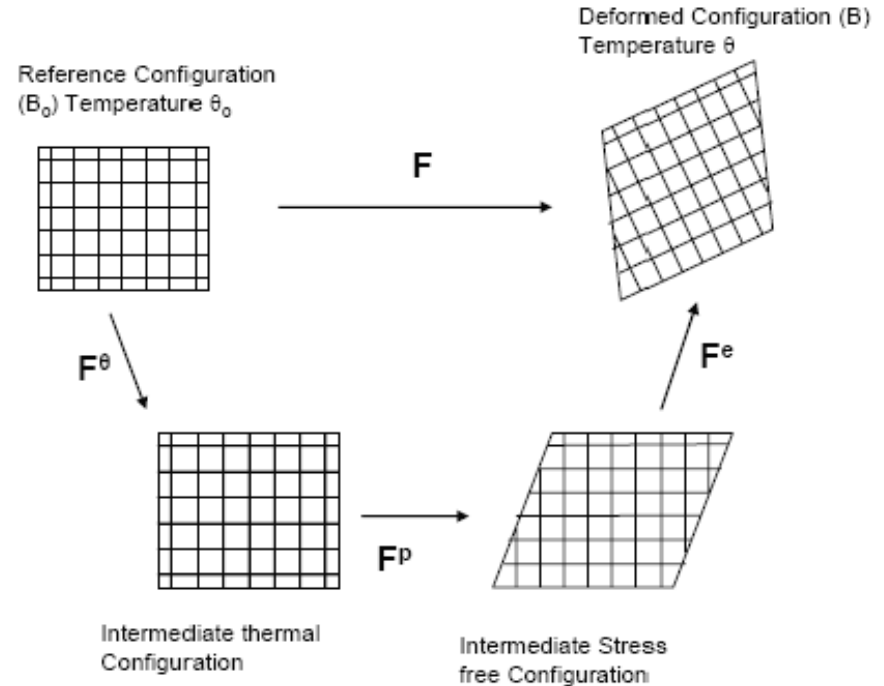
$$\mathbf{F} = \frac{\partial \mathbf{x}}{\partial \mathbf{X}} = \mathbf{F}^e \cdot \mathbf{F}^p \cdot \mathbf{F}^\theta$$

Velocity gradient

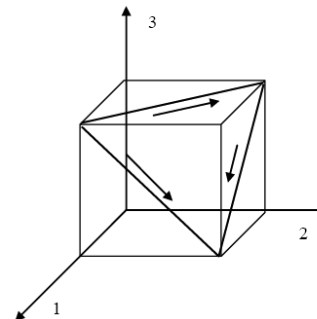
$$\mathbf{L} = \dot{\mathbf{F}} \cdot \mathbf{F}^{-1}$$

Macroscopic plastic velocity gradient

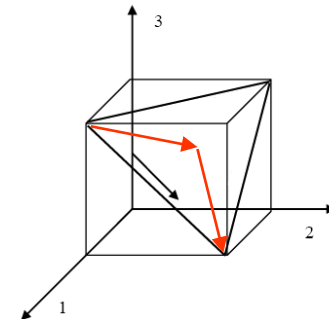
$$\mathbf{L}^p = \dot{\mathbf{F}}^p \cdot \mathbf{F}^{p-1} = \sum_{\alpha=1}^{N_{slip}} \dot{\gamma}^{(\alpha)} \left(\mathbf{s}_o^{(\alpha)} \otimes \mathbf{n}_o^{(\alpha)} \right)$$



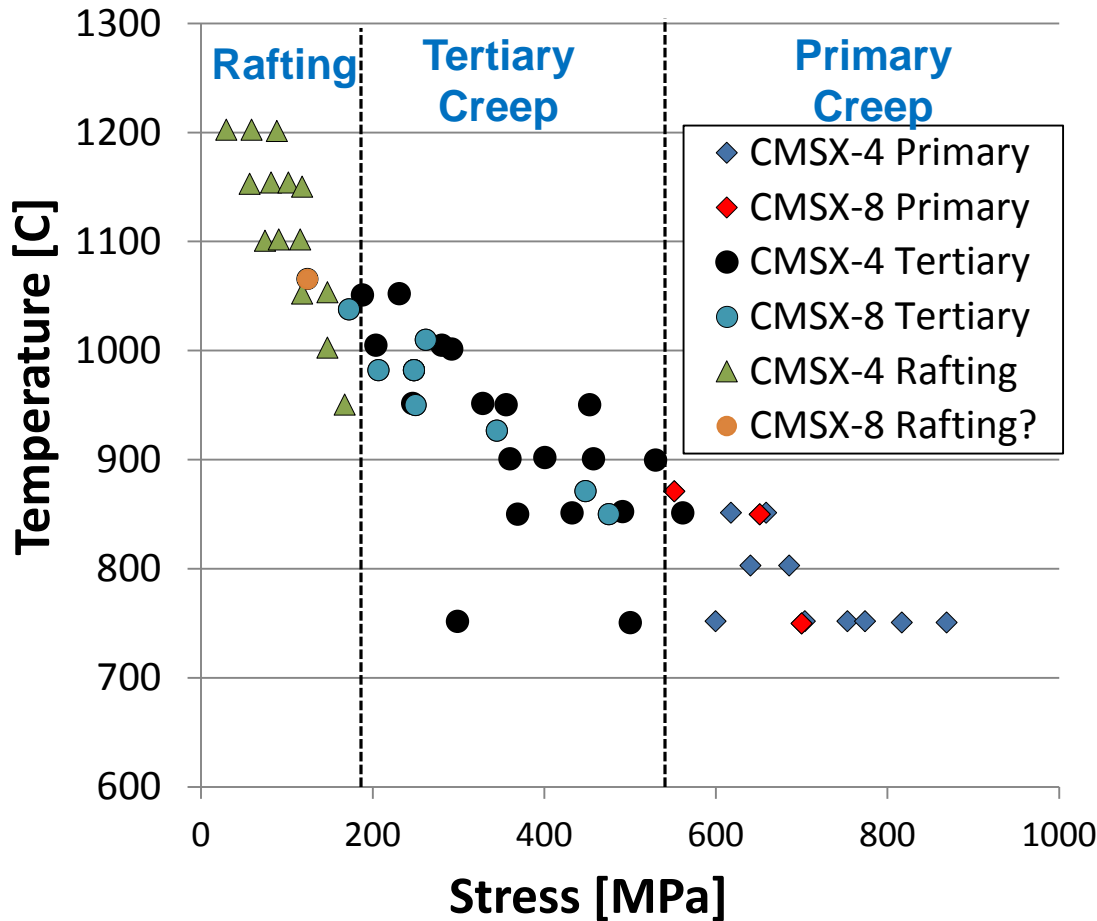
In γ : 12 octahedral slip systems active



In γ' : 12 octahedral slip systems moving as dislocation ribbons

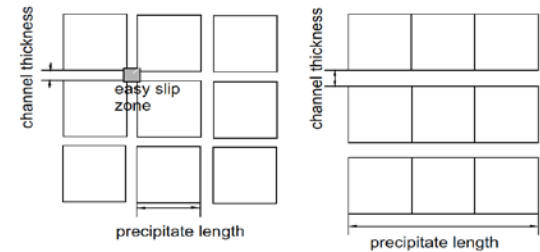


Influence of stress and temperature on modes of creep deformation



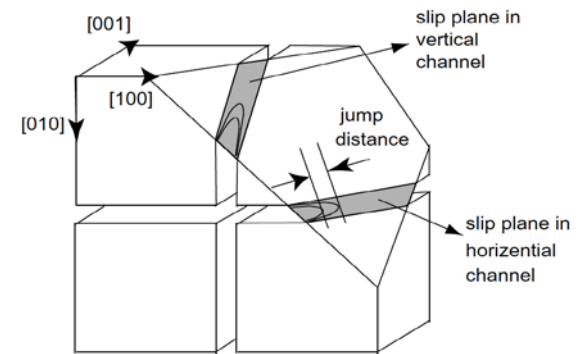
[Reed, 2006; Ma, Dye, and Reed, 2008, CMSX-8 Data]

Rafting – transport of matter constituting the γ phase out of the vertical channels and into the horizontal ones (tensile creep case)



[Ma, Dye, and Reed, 2008]

Tertiary – dislocation activity restricted to $a/2\langle 110 \rangle$ form operating on $\{111\}$ slip planes in the γ channels



[Ma, Dye, and Reed, 2008]

Primary – γ' particles are sheared by dislocation ribbons of overall Burgers vector $a\langle 112 \rangle$ dissociated into superlattice partial dislocations separated by a stacking fault; shear stress must above threshold stress (about 550 MPa)

Inelastic Velocity Gradient

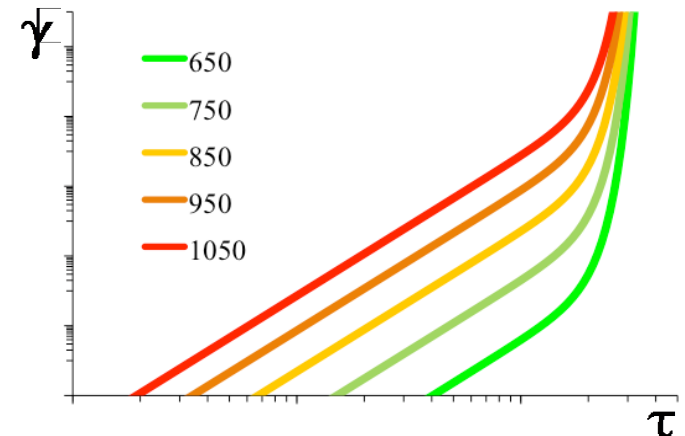
$$\mathbf{L}^{in} = \dot{\mathbf{F}}^{in} \mathbf{F}^{in-1} = f_{\gamma} \left(\sum_{\alpha=1}^{12} \dot{\gamma}_{\gamma}^{in(\alpha)} \left(\hat{\mathbf{d}}^{(\alpha)} \otimes \hat{\mathbf{n}}^{(\alpha)} \right) \right) + f_{\gamma'} \left(\sum_{\alpha=13}^{24} \dot{\gamma}_{L1_2}^{in(\alpha)} \left(\hat{\mathbf{d}}^{(\alpha)} \otimes \hat{\mathbf{n}}^{(\alpha)} \right) \right)$$

Inelastic Shear Strain Rate

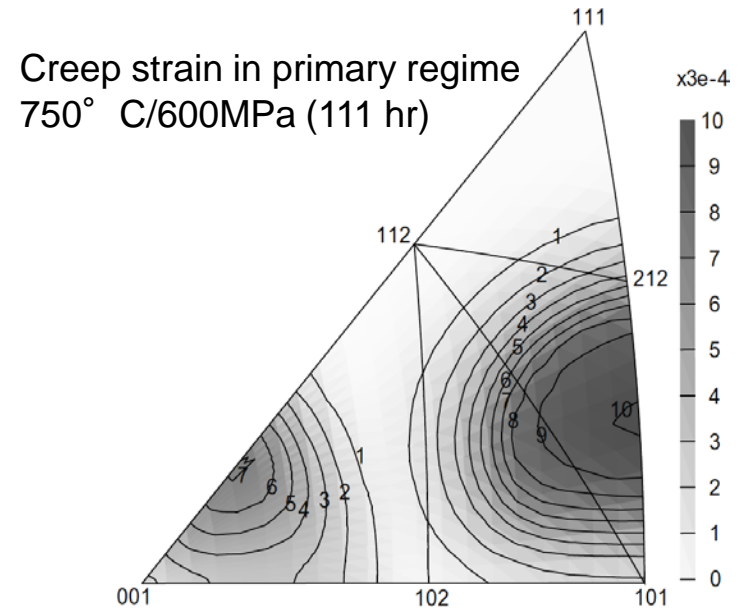
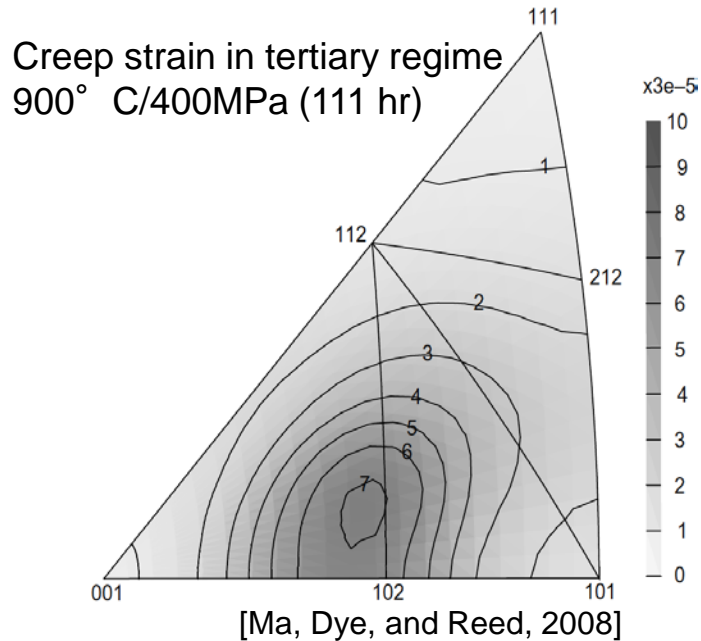
$$\left\{ \begin{aligned} \dot{\gamma}_{\gamma}^{in(\alpha)} &= \rho_{\gamma}^{(\alpha)} b \lambda_{\gamma}^{(\alpha)} F_{attack} \text{sign} \left(\tau^{(\alpha)} + \tau_{mis}^{(\alpha)} - \chi^{(\alpha)} \right) \exp \left\{ \frac{-Q_{slip}^{110} + \left(\left| \tau^{(\alpha)} + \tau_{mis}^{(\alpha)} - \chi^{(\alpha)} \right| - \tau_{\gamma pass}^{(\alpha)} - \tau_{oro}^{(\alpha)} \right) V_{c1}^{(\alpha)}}{kT} \right\} \\ \dot{\gamma}_{L1_2}^{in(\alpha)} &= \rho_{L1_2}^{(\alpha)} b \lambda_{L1_2}^{(\alpha)} F_{attack} \text{sign} \left(\tau^{(\alpha)} - \chi^{(\alpha)} \right) \exp \left\{ \frac{-Q_{slip}^{112} + \left(\left| \tau^{(\alpha)} - \chi^{(\alpha)} \right| - \tau_{L1_2 pass}^{(\alpha)} - \tau_{APB} \right) V_{c2}^{(\alpha)}}{kT} \right\} \end{aligned} \right.$$

Evolution Equations

$$\left\{ \begin{aligned} \dot{\rho}_{\gamma}^{(\alpha)} &= \frac{1}{b} \left(\frac{c_{mult1}}{\lambda_{\gamma}^{(\alpha)}} - c_{annh1} \rho_{\gamma}^{(\alpha)} \right) \left| \dot{\gamma}_{\gamma}^{in(\alpha)} \right| \\ \dot{\rho}_{L1_2}^{(\alpha)} &= c_{mult21} \rho_{pb}^{(\alpha)} \Gamma + \frac{c_{mult22}}{b \lambda_{\gamma'}^{(\alpha)}} \left| \dot{\gamma}_{\gamma'}^{(\alpha)} \right| - c_{annh2} \rho_{\gamma'}^{(\alpha)} \left| \dot{\gamma}_{\gamma'}^{(\alpha)} \right| \\ \dot{\rho}_{pb}^{(\alpha)} &= \frac{c_{mult}^{pb}}{b L_{\gamma}} \left| \dot{\gamma}_{\gamma}^{in(\alpha)} \right| - c_{annh}^{pb} \rho_{pb}^{(\alpha)} \left| \dot{\gamma}_{\gamma}^{in(\alpha)} \right| \end{aligned} \right.$$

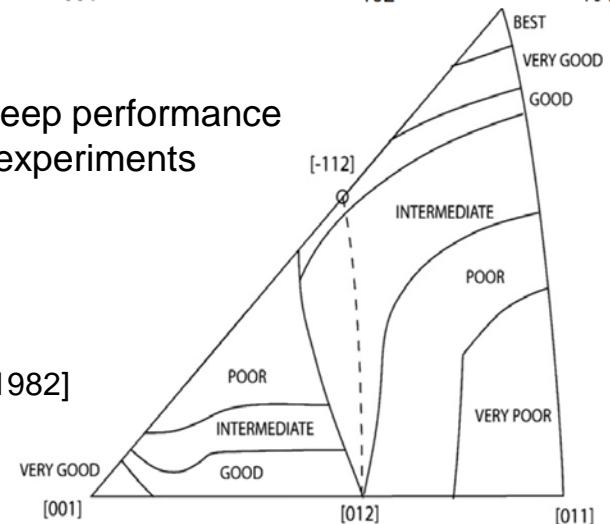


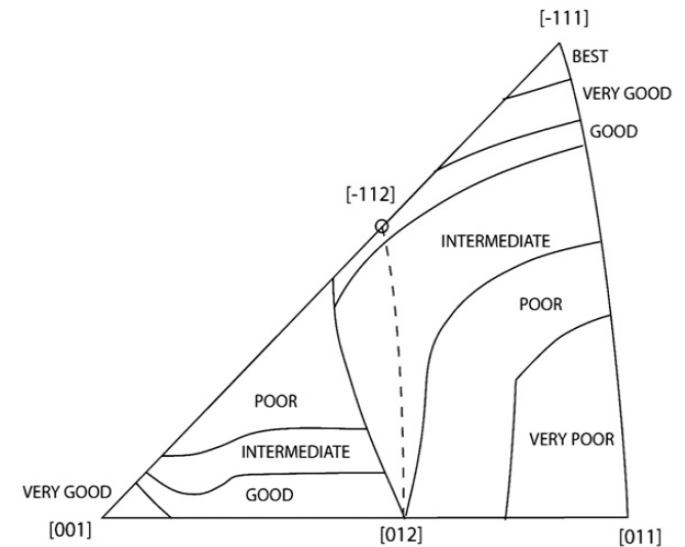
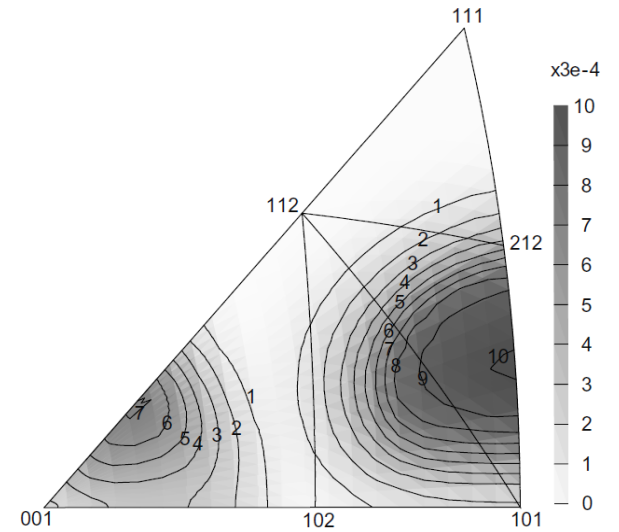
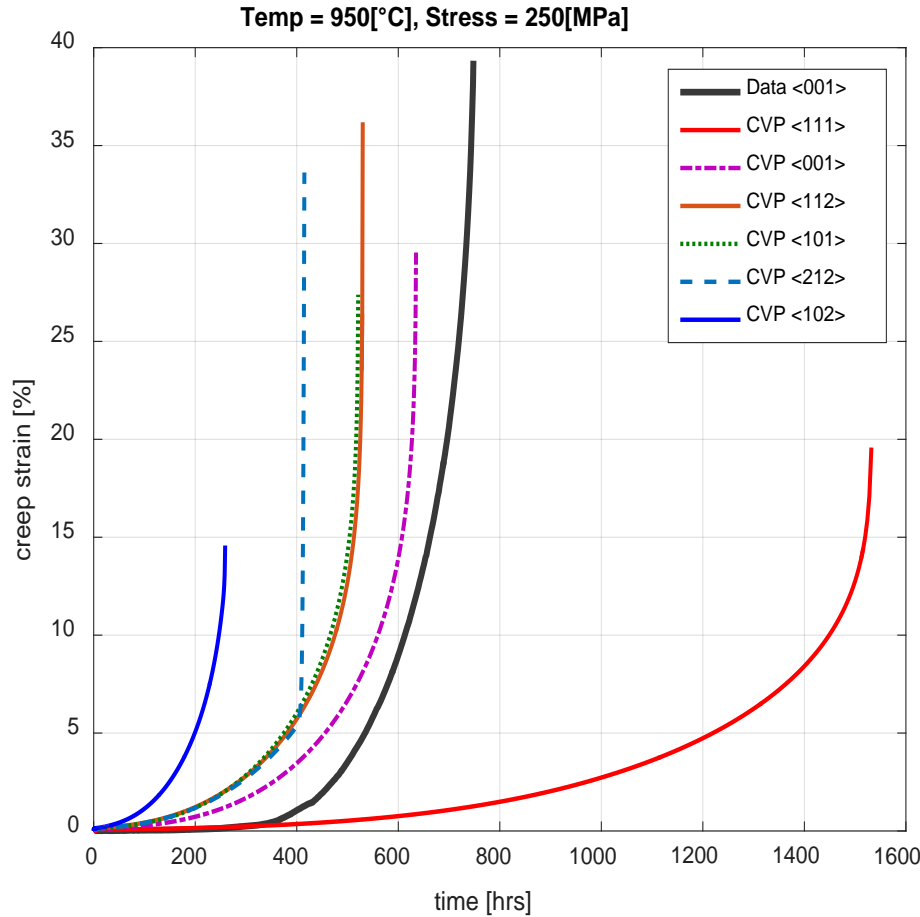
CMSX-4 Model Predictions



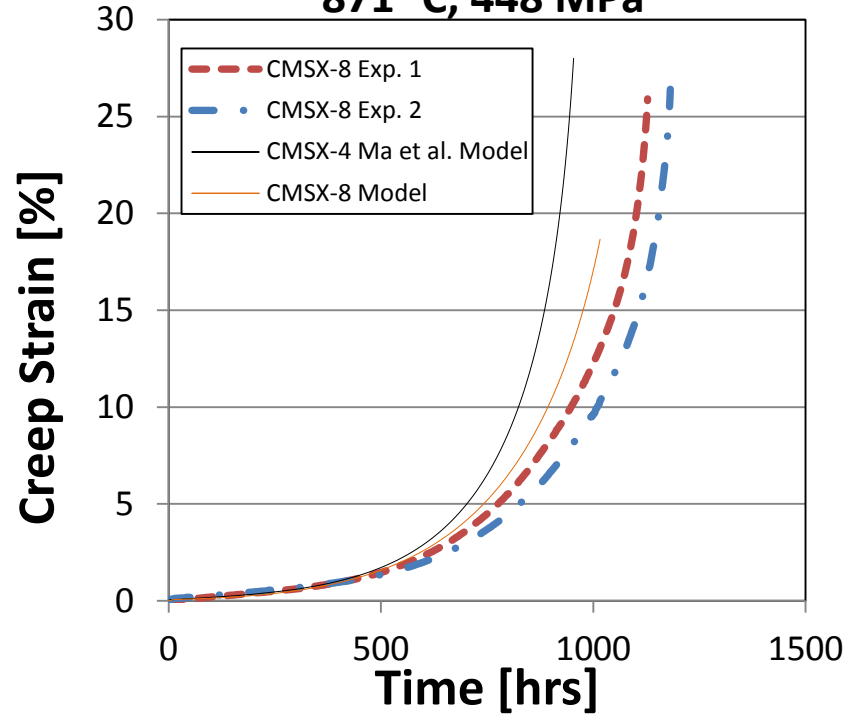
Primary creep performance based on experiments

[MacKay and Meier, 1982]

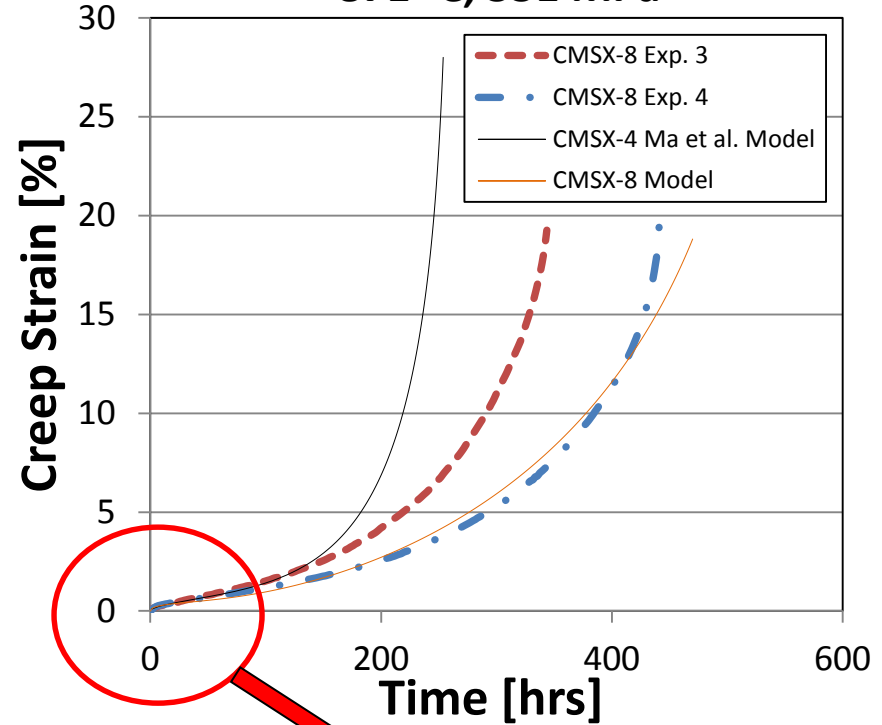




871 °C, 448 MPa

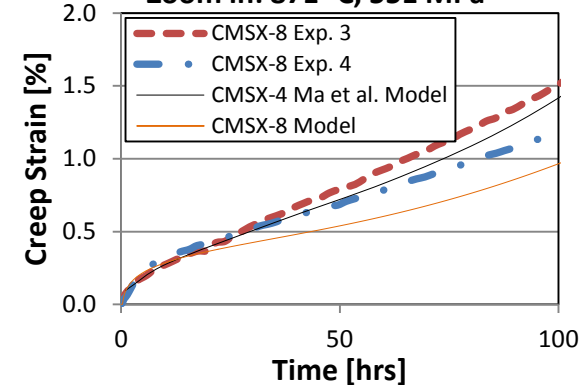


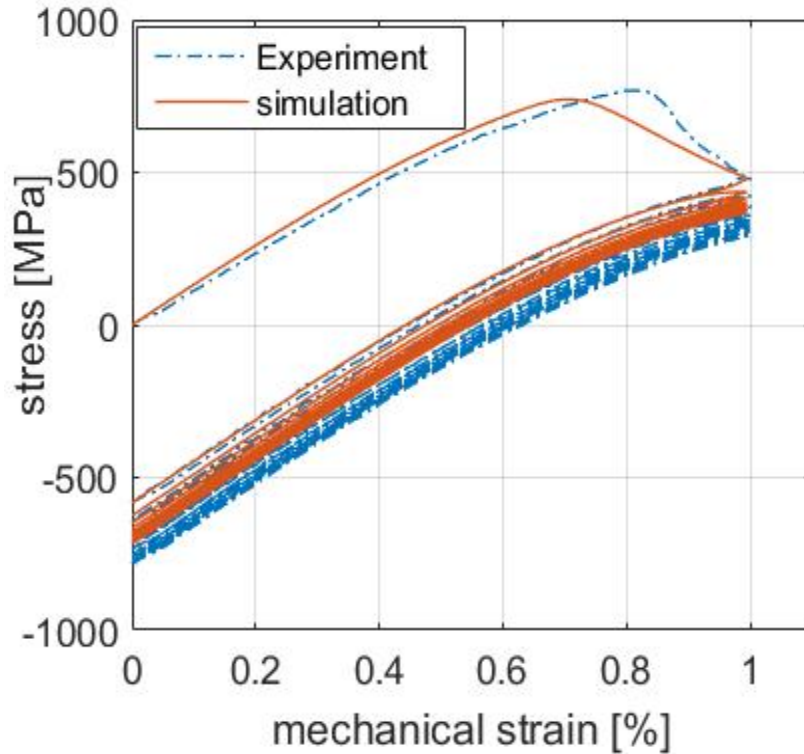
871 °C, 551 MPa



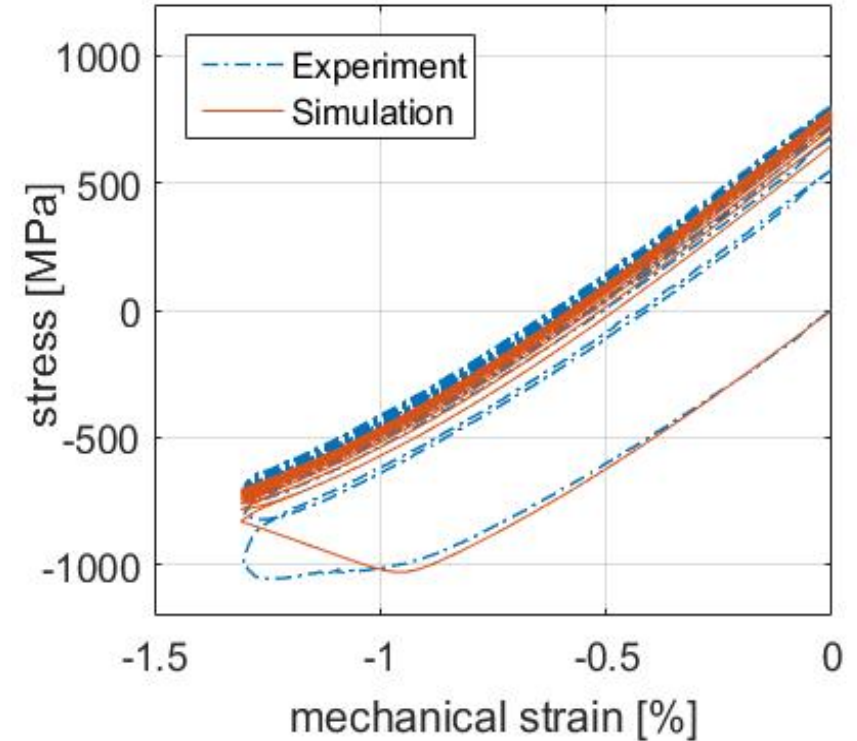
Primary, secondary and tertiary creep can be captured with the model

Zoom in: 871 °C, 551 MPa



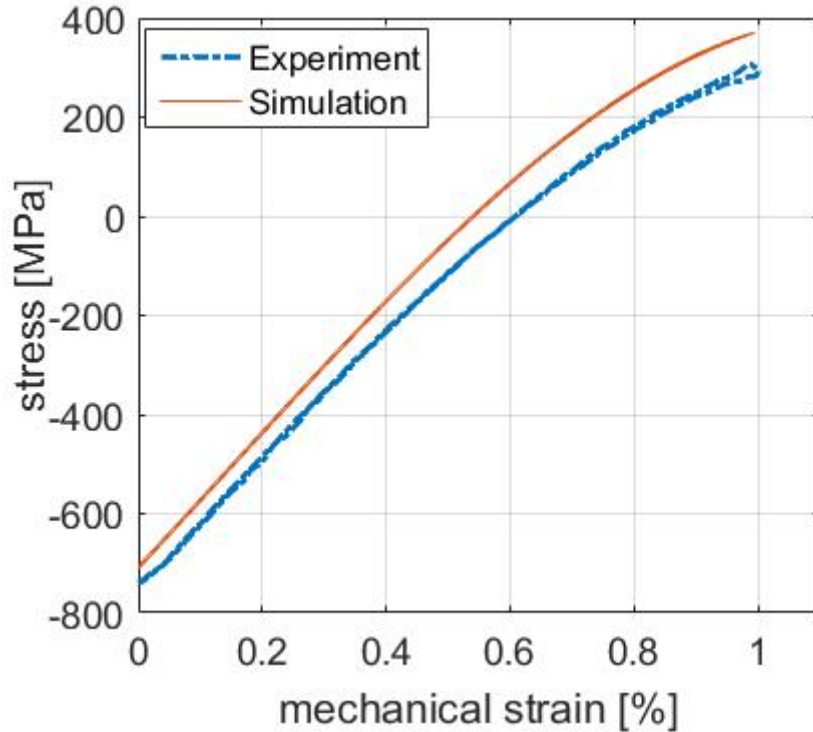


First 10 cycles: IP-TMF
 [100-1100-100] °C, $R = 0$, $\dot{T} = 2.83$ [°K/s]

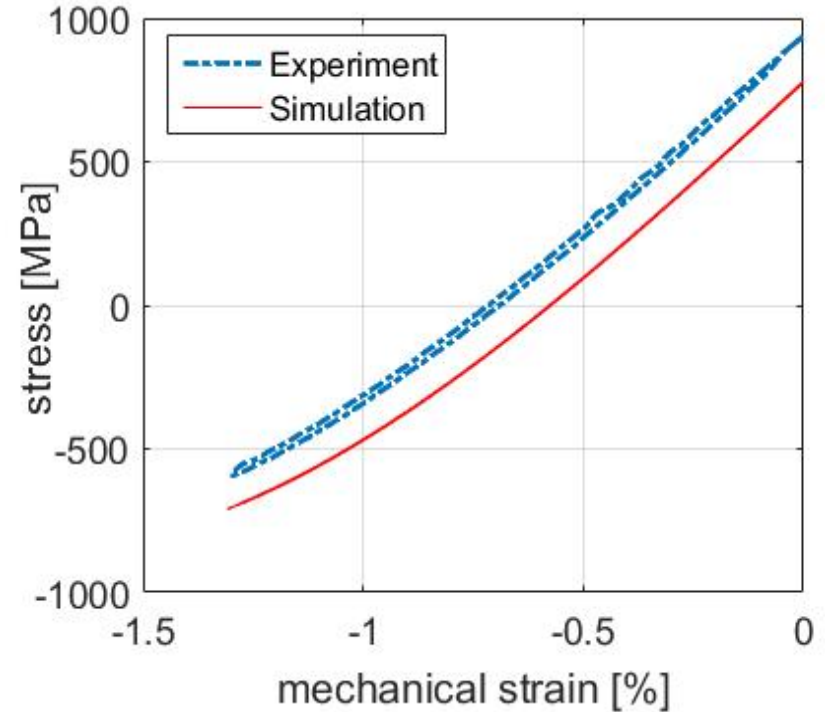


Stabilized hysteresis: OP-TMF
 [100-850-100] °C, $R = -\infty$, $\dot{T} = 2.83$ [°K/s]

Very good agreement predicting TMF



Stabilized hysteresis: IP-TMF
 [100-1100-100] °C, $R = 0$, $\dot{T} = 2.83$ [°K/s]



Stabilized hysteresis: OP-TMF
 [100-850-100] °C, $R = -\infty$, $\dot{T} = 2.83$ [°K/s]

Very good agreement predicting TMF

Since Re segregates almost exclusively in the γ channels, the Activation energy in the γ phase can be modified to account for Re content as follows:

$$\left\{ \begin{array}{l} \dot{\gamma}_{\gamma}^{in(\alpha)} = \Theta(T) \rho_{\gamma}^{(\alpha)} b \lambda_{\gamma}^{(\alpha)} F_{attack} \text{sign}(\tau^{(\alpha)} + \tau_{mis}^{(\alpha)} - \chi^{(\alpha)}) \exp \left\{ \frac{-Q_{slip}^{110} + \left(\left| \tau^{(\alpha)} + \tau_{mis}^{(\alpha)} - \chi^{(\alpha)} \right| - \tau_{\gamma pass}^{(\alpha)} - \tau_{oro}^{(\alpha)} \right) V_{c1}^{(\alpha)}}{kT} \right\} \\ \dot{\gamma}_{Ll_2}^{in(\alpha)} = \rho_{Ll_2}^{(\alpha)} b \lambda_{Ll_2}^{(\alpha)} F_{attack} \text{sign}(\tau^{(\alpha)} - \chi^{(\alpha)}) \exp \left\{ \frac{-Q_{slip}^{112} + \left(\left| \tau^{(\alpha)} - \chi^{(\alpha)} \right| - \tau_{Ll_2 pass}^{(\alpha)} - \tau_{APB} \right) V_{c2}^{(\alpha)}}{kT} \right\} \end{array} \right.$$

If we considering activation energy for plastic flow Q_o a function of %Re, the diffusivity parameter could take the form of:

$$\Theta(T) = \exp\left(-\frac{Q_o}{RT}\right) \quad \text{for } T \geq \frac{T_m}{2} \qquad \Theta(T) = \exp\left(-\frac{2Q_o}{RT} \left[\ln\left(\frac{T_m}{2T}\right) + 1 \right]\right) \quad \text{for } T \leq \frac{T_m}{2}$$

- Exercise new CVP codes
 - (1) displacement-controlled algorithm coded in FORTRAN as UMAT for ABAQUS (suitable for 3D analysis of detailed features, but computationally expensive)
 - (2) stress-controlled algorithm coded in MATLAB (limited to 1D loadings, but computationally cheap; utility in alloy design; early design iterations)
- Characterize aged microstructure and its analysis
 - Establish protocols for reduced-order modeling of the current state of the microstructure using spatial correlations and principal component analysis
 - Develop PSP linkage models using PC values for describing current state of the microstructure
- Creep-fatigue interaction life analysis relationships using all new data
- Disseminate research
 - Archival journal articles
 - Intern with Siemens Energy
 - Workshops and Conferences (UTSR, ASME, ...)
- Ernesto Estrada Rodas – complete Ph.D. studies in 2017